

On the Algorithmic Power of Spiking Neural Networks

Chi-Ning Chou*, Kai-Min Chung[†] and Chi-Jen Lu[‡]

December 14, 2024

Abstract

Spiking Neural Networks (SNN) are mathematical models in neuroscience to describe the dynamics among a set of neurons which interact with each other by firing spike signals to each other. Interestingly, recent works observed that for an *integrate-and-fire* model, when configured appropriately (e.g., after the parameters are learned properly), the neurons' *firing rate*, i.e., the average number of spikes fired per unit of time for each neuron, converges to an optimal solution of Lasso and certain quadratic optimization problems. Thus, SNN can be viewed as a natural algorithm for solving such convex optimization problems. However, theoretical understanding of SNN algorithms remains limited. In particular, only the convergence result for the Lasso problem is known, but the bounds of the convergence rate remain unknown. Therefore, we do not know any explicit complexity bounds for SNN algorithms.

In this work, we investigate the algorithmic power of the integrate-and-fire SNN model after the parameters are properly learned/configured. In particular, we explore what algorithms SNN can implement. We start by formulating a clean discrete-time SNN model to facilitate the algorithmic study. We consider two SNN dynamics and obtain the following results.

- We first consider an arguably simplest SNN dynamics with a threshold spiking rule, which we call simple SNN. We show that simple SNN solves the least square problem for a matrix $A \in \mathbb{R}^{m \times n}$ and vector $\mathbf{b} \in \mathbb{R}^m$ with timestep complexity $O(\kappa n/\varepsilon)$, where κ is the condition number of $A^\top A$ and ε is the relative error.
- For the under-determined case, we observe that simple SNN may solve the ℓ_1 minimization problem (i.e., find \mathbf{x} that satisfies $A\mathbf{x} = \mathbf{b}$ with the minimal ℓ_1 norm) using an interesting *primal-dual* algorithm, which solves the dual problem by a gradient-based algorithm while updates the primal solution along the way. We do not know how to analyze it, so we analyze a variant dynamics and use simulation to serve as partial evidence to support the conjecture. Our simulation shows that simple SNN achieves comparable efficiency under random instances as ℓ_1 -magic, a practical solver for the ℓ_1 minimization problem.
- We also consider SNN with a stochastic spiking rule and show that it implements a natural stochastic gradient descent algorithm to solve the least square problem. An interesting point here is that we do not need to assume that $A^\top A$ is full rank, so the objective function may not be strongly convex, a condition usually required by stochastic gradient algorithms. The reason is that stochastic SNN can implicitly execute the stochastic gradient algorithm in the range space of $A^\top A$, where the objective function becomes strongly convex.

*School of Engineering and Applied Sciences, Harvard University, USA.

[†]Institute of Information Science, Academia Sinica, Taipei, Taiwan.

[‡]Institute of Information Science, Academia Sinica, Taipei, Taiwan.

1 Introduction

Natural algorithms aim to understand and explain the algorithms observed in natural systems or dynamics. Seminal works such as bird flocking [Cha09, Cha12], slime systems [NYT00, TKN07, BMV12], and evolution [LPR⁺14, LP16] successfully discover the underlying algorithmic ideas of different natural objects. These examples not only discover new algorithmic insights but also inspire new mathematical tools and models. In this work, we are interested in the algorithmic power of the *spiking neural networks (SNN)* as natural algorithms for solving convex optimization problems. We focus on the computational aspect of SNN instead of the learning aspect; that is, we treat the synapses (connectivities between neurons) as given in advance (e.g. after the parameters are learned properly), and aim to understand how SNN solves computational problems both qualitatively and quantitatively.

In general, a SNN refers to a set of neurons that can send signals to each other by spikes through their synaptic connections (i.e., edges between two neurons). There has been rich literature in neuroscience searching for mathematical models to explain and predict various (statistical) behaviors of different types of SNN [I⁺03, Adr26, Lap07]. Here, we focus on the integrate-and-fire model, where, roughly speaking, each neuron is associated with a time-varying *potential* value and receives a steady rate of external charging to its potential as an environmental input. When a neuron’s potential exceeds a certain threshold, it fires a spike to other neurons (and affects their potentials) and its potential drops instantaneously. Integrate-and-fire model is one of the earliest neuron models proposed by Lapicque [Lap07] and is the foundation of many later models.

Because of the steady external charging, a SNN dynamic will not converge to a fix state. Rather, the neurons will continue to fire spikes to each other. An important statistic is the neuron’s firing rate, which is the average number of spikes fired by each neuron per unit of time. Barrett et al. [BDM13] investigated the firing rate of a certain class of SNN. Interestingly, they observed that the firing rate can be characterized as the optimal solution of certain quadratic programming problems defined by the parameters of the SNN. Barrett et al. further mentioned that the SNN dynamics can be viewed as an algorithm to solve the corresponding optimization problem. However, no rigorous analysis was given in their work.

SNN dynamics is also considered in a different context to simulate the so-called *locally competitive algorithms (LCA)* [RJBO08] for solving the Lasso (least absolute shrinkage and selection operator) optimization problem¹, which is widely used in statistical modeling. Roughly speaking, LCA is also a dynamics among a set of neurons, but unlike in SNN, where the neurons fire discrete spike signals, in LCA, the neurons continuously signal their potential values (or a function of the values) to their neighboring neurons, which is more expensive to implement than discrete spikes. Another difference is that the neurons’ potentials in LCA will converge to a fixed value, which is the output of the algorithm. In contrast, in SNN, only the neurons’ firing rates may converge instead of their potentials.

Motivated by the efficiency consideration, Shapero et al. [SRH13, SZHR14] proposed to use a SNN dynamics called *spike LCA (S-LCA)* to replace the continuous signals by discrete spikes and to use the firing rate of S-LCA as output. Recently, Tang et al. [TLD17] showed that the firing rate of S-LCA indeed converges to a variant of Lasso problem² in the limit. These works also

¹Note that Lasso is equivalent to the Basis Pursuit De-Noising (BPDN) program under certain parameters transformation.

²In this variant, all the entries in matrix A is non-negative.

experimentally demonstrated the efficient convergence of S-LCA and its advantage of fast identifying sparse solutions with potentially competitive practical performance to other Lasso algorithms (e.g., FISTA [BT09]). However, there is no proof of convergence rate, and thus we do not know any explicit complexity bound of S-LCA.

Viewing a SNN dynamics as a natural algorithm, it can be viewed as a simple distributed algorithm that is highly parallelizable. Indeed, each neuron can be viewed as a distributed node performing simple update operations in parallel. The inter-neuron interactions are spike signals, which can be implemented with extremely simple communications (just sending the spike signals). For a SNN dynamics, we can define the timestep and spike complexity as the number of timesteps and spikes it takes to solve the optimization problem (see below for formal definitions), which naturally corresponds to the parallel and total time complexity when one implements the SNN dynamics as a (parallel/distributed) algorithm. The spike complexity can also be viewed as the energy cost of the SNN dynamics. As we shall see, SNN dynamics have the potential to yield energy and time efficient parallel algorithms for optimization problems.

We are intrigued by the power of SNN as a simple distributed algorithm for solving complex optimization problems with potentially competitive theoretical and/or practical performances. In this work, we investigate the algorithmic power of SNN dynamics by exploring the following three directions.

Question 1. *What algorithms can SNN implement?*

Shapero et al. [SRH13, SZHR14] showed that SNN can implement LCA, which in turn can be viewed as a gradient-based algorithm. What else?

Question 2. *What optimization problems can SNN solve?*

Shapero et al. [SRH13, SZHR14] and Tang et al. [TLD17] showed that SNN can solve Lasso, and Barrett et al. [BDM13] observed that SNN can solve certain quadratic optimization problems. What else?

Question 3. *What is the parallel time complexity and spike complexity of the SNN algorithms?*

To the best of our knowledge, there is no proof of complexity bound for any SNN algorithm. Can we prove explicit complexity bounds for some SNN algorithms?

1.1 Our Contributions

To investigate the power of SNN for solving optimization problems, our starting point is to formulate a clean *discrete-time* SNN model — we choose to work with the discrete-time model because it has concrete complexity measures. Specifically, a SNN dynamics with n neurons is described by the vector $\mathbf{u}(t) \in \mathbb{R}^n$ of the neurons’ potential at each timestep $t \in \mathbb{N}$. We assume that initially $\mathbf{u}(1) = 0$, and the dynamics is described by the following equation for every timestep $t \in \mathbb{N}$.

$$\mathbf{u}(t + 1) = \mathbf{u}(t) - \alpha \cdot C\mathbf{s}(t) + \mathbf{I} \cdot \Delta t, \tag{1}$$

where

- The $\mathbf{I} \cdot \Delta t$ term describes the (constant) *external charging rule* of the dynamics. Specifically, each neuron may receive a constant potential from its local external charging, where $\mathbf{I} \in \mathbb{R}^n$

describes the amount of potential (which can be positive or negative) the neurons receive per unit of time. Δt is a timestep size parameter describe the elapsed time of a timestep. Thus, each neuron i is charged by $\mathbf{I}_i \cdot \Delta t$ potential per timestep.

- The $-\alpha \cdot C s(t)$ term describes the inter-neuron spike interaction. Specifically, $\mathbf{s}(t) \in \{-1, 0, 1\}^n$ records whether each neuron fires a spike at timestep t . We consider (non-standard) *two-sided* spikes,³ where the value $\mathbf{s}_i(t) \in \{-1, 0, 1\}$ indicates that neuron i fires a negative spike, no spike, or a positive spike at timestep t , respectively. Whether a neuron fires is determined by applying a *spiking rule function* $R : \mathbb{R} \rightarrow \{-1, 0, 1\}$ (possibly randomized) to its potential, i.e., $\mathbf{s}_i(t) = R(\mathbf{u}_i(t))$. Typically, R is a certain form of threshold rule saying that a neuron fires if its potential exceeds a certain threshold η . $C \in \mathbb{R}^{n \times n}$ is a *connectivity matrix* that describes how does a neuron react to a spike from another neuron, and $\alpha \in \mathbb{R}$ is the spiking strength parameter. When neuron i fires at timestep t , the potential of each neuron j is updated by $-\alpha \cdot C_{ij} \cdot \mathbf{s}_i(t)$. Thus, positive (resp., negative) C_{ij} corresponds inhibition (resp., exhibition) effect.

A SNN dynamics is specified by the external charging vector \mathbf{I} , the connectivity matrix C , the spiking rule function R , and the parameters α and Δt . Here we think of \mathbf{I} and C as given parameters (e.g., after learned or configured properly) instead of varying ones in the SNN model. An important statistics of the dynamics is the *firing rate* defined as $\mathbf{x}_i(t) := \left(\sum_{1 \leq s \leq t} \mathbf{s}_i(s) \right) / (t \cdot \Delta t)$ for neuron $i \in [n]$ at timestep t , namely, the average number of spikes per unit of time for neuron i up to timestep t .

We study *SNN algorithms* that solve optimization problems by configuring a SNN dynamics, simulating it for certain number of timesteps T , and outputting the firing rate $\mathbf{x}(T)$ as a solution of the problem. Clearly, such algorithms have the advantage of being easily parallelized or implemented as distributed algorithms. Note that the complexity of such algorithms is determined by the number of timesteps T , referred to as the *timestep complexity*, and the number of spikes $S := \sum_{1 \leq t \leq T} \sum_{i \in [n]} |\mathbf{s}_i(t)|$ fired in the dynamics, referred to as the *spike complexity*. Specifically, $O(n \cdot (T + S))$ (resp., $O(T + S)$) is the time complexity (resp., parallel time complexity) to simulate the dynamics. When implemented as a distributed algorithm T corresponds to the round complexity and $O(n \cdot S)$ corresponds to the communication complexity.

We refer the readers to Section 3 for further discussion of our model and its comparison with SNN models in the literature. In the following, we present our results on SNN algorithms.

Simple SNN solves the least square problem. We start by investigating the power of a *simple SNN* with a basic threshold spiking rule $R = R_\eta$ for some threshold parameter $\eta > 0$, where $R_\eta(u) = 1$ if $u > \eta$, $R_\eta(u) = -1$ if $u < -\eta$, and $R_\eta(u) = 0$ otherwise. Namely, a neuron fires if its potential exceeds the threshold $\pm\eta$. This is arguably the simplest SNN dynamics one can consider. Our first result show that, when properly configured, simple SNN solves the least square problem.

Recall that given a matrix $A \in \mathbb{R}^{m \times n}$ and a vector $\mathbf{b} \in \mathbb{R}^m$, the goal of the least square problem is to find $\mathbf{x} \in \mathbb{R}^n$ that minimizes $\|\mathbf{b} - A\mathbf{x}\|_2^2/2$. To solve the least square problem, we configure a simple SNN with n neurons with connectivity matrix $C = A^\top A$ and external charging vector

³We emphasize that our goal is not to capture the biological neurons but to investigate the algorithmic power of SNN. The non-standard choice of two-sided spike model facilitates the algorithmic study in that it helps to configure SNN algorithms with cleaner analysis. We also note that the two-sided spike model is not stronger in the sense that it can be simulated by the standard one-sided model. We give a thorough discussion of our model in Section 3.2.

$\mathbf{I} = A^\top \mathbf{b}$. We show that when the parameters $\alpha, \eta, \Delta t$ are set properly, the residual error of the firing rate to the least square problem will converge to zero.

Theorem 1 (informal). *Given $A \in \mathbb{R}^{m \times n}$, $\mathbf{b} \in \mathbb{R}^m$, and $\epsilon > 0$. Let $\mathbf{x}(t)$ be the firing rate of the above simple SNN with $\eta \geq \lambda_{\max}$ and $\Delta t \leq \frac{\sqrt{\lambda_{\min}}}{24\sqrt{n}\|\mathbf{b}_A\|_2}$ where \mathbf{b}_A is the projection of \mathbf{b} on the range space of A . When $t \geq \frac{48\kappa n}{\epsilon}$, $\mathbf{x}(t)$ is an ϵ -approximate solution⁴ for the least square problem of (A, \mathbf{b}) , where κ is the condition number of $A^\top A$ ⁵. Specifically, the timestep complexity of the simple SNN to produce an ϵ -approximate solution is $T = O(\frac{\kappa n}{\epsilon})$.*

The theorem implies that simple SNN solves the least square problem with relative error ϵ in timestep complexity $O(\kappa n/\epsilon)$. To the best of our knowledge, this is the first result proving an explicit complexity bound for SNN dynamics as algorithms for solving optimization problems.⁶ On the other hand, we note that here we need the information of λ_{\max} and λ_{\min} , which are defined as the maximum and the minimum nonzero eigenvalue of $A^\top A$ respectively, to configure the SNN. As a result, it is only applicable when a good estimation of the parameters are known (the algorithm works when $\eta \geq \lambda_{\max}$ and $\Delta t \leq \frac{\sqrt{\lambda_{\min}}}{24\sqrt{n}\|\mathbf{b}_A\|_2}$).

We note that the dependency of simple SNN on n is interesting in the following two ways. First, the timestep complexity is optimal for dense matrix with n parallel processors. The reason is that an algorithm must access every entry, which is $\Omega(n^2)$ and there are n neurons so the parallel running time is $\Omega(n)$. Second, define the parallel continuous time complexity to be $T \cdot \Delta t$ to capture the total amount of the external charging \mathbf{b} that have been injected into each neuron. The parallel continuous time complexity of simple SNN is then $T \cdot \Delta t = O(\sqrt{n})$, which is *sub-linear* in n . That is, for a single neuron i , only $O(\sqrt{n})$ amount of the external charging \mathbf{b}_i is required.

Let us sketch out an informal argument here to see why the residual error will converge to zero. An important fact to note is that the neurons' potential $\mathbf{u}(t)$ will remain bounded. Now, note that the potential is only affected by the constant external charging $\mathbf{I} \cdot \Delta t = A^\top \mathbf{b} \cdot \Delta t$ and the spike $-A^\top A \cdot \mathbf{s}$. Intuitively, for the potential to remain bounded, the constant external charging needs to be balanced by the effect of the spikes over time. Let \mathbf{x} denote the firing rate of simple SNN, we should expect that $A^\top A \cdot \mathbf{x} \approx A^\top \mathbf{b}$. Namely, the average effect of the spike should roughly be the external charging for one unit of time. As the residual error of the firing rate is $\|\mathbf{b} - A\mathbf{x}\|_2^2/2$, the above discussion means that the gradient of $\|\mathbf{b} - A\mathbf{x}\|_2^2$ will converge to zero, which implies the optimality of \mathbf{x} .

Stochastic SNN as a stochastic gradient descent algorithm. We next consider SNN with *stochastic* spiking rules, i.e., the decision of firing is randomized. Stochastic spiking rules are considered in the literature (e.g., [Maa14, Maa15, JHM16]), but in different contexts (not for solving convex optimization problems). We show that by properly configuring a stochastic SNN dynamics, the dynamics implement a natural stochastic gradient descent algorithm for solving the least square problem.

Specifically, we consider the following *stochastic threshold spiking rule* $R_\eta^{\text{stochastic}} : \mathbb{R} \rightarrow \{-1, 0, 1\}$,

⁴The ϵ -approximate notion is the standard error measure in this context. See Section 2 for formal definition.

⁵Please refer to Section 2 for formal definitions.

⁶As far as we know, previous results (e.g., [TLD17]) only proved convergence results when the time goes to infinity without an explicit time bound.

for some threshold parameter $\eta > 0$, defined as follows.

$$R_\eta^{\text{stochastic}}(u) = \begin{cases} \text{sgn}(u) & , \text{ with probability } \min\{\frac{|u|}{\eta}, 1\} \\ 0 & , \text{ with probability } 1 - \min\{\frac{|u|}{\eta}, 1\}. \end{cases} \quad (2)$$

In other words, the probability that a neuron fires is proportional to the magnitude of its potential and a neuron fires with certainty if the magnitude of its potential exceeds η . We refer to SNN with this spiking rule as *stochastic SNN*.

Given an instance $A \in \mathbb{R}^{m \times n}$ and $\mathbf{b} \in \mathbb{R}^m$ of the least square problem, we configure a stochastic SNN with n neurons with connectivity matrix $C = A^\top A$ and external charging vector $\mathbf{I} = A^\top \mathbf{b}$, and set $\alpha = 1$ as before. To implement stochastic gradient descent, we set $\Delta t = 1/\eta$ (we leave η to be determined later). The dynamics is described by the following equation for $t \in \mathbb{N}$.

$$\mathbf{u}(t+1) = \mathbf{u}(t) - A^\top A \cdot \mathbf{R}_\eta^{\text{stochastic}}(\mathbf{u}(t)) + A^\top \mathbf{b} \cdot \Delta t. \quad (3)$$

Assuming $\|\mathbf{u}(t)\|_\infty \leq \eta$, the expectation $\mathbb{E}[\mathbf{R}_\eta^{\text{stochastic}}(\mathbf{u}(t))] = \mathbf{u}(t)/\eta$, so the expected update of \mathbf{u} is $-(A^\top A \mathbf{u}(t) - A^\top \mathbf{b})/\eta$, which is indeed the gradient direction of the objective function $\|\mathbf{b} - A\mathbf{u}\|_2^2/2$. Therefore, when η is set sufficiently large, the dynamics of stochastic SNN implements a stochastic gradient descent algorithm for the least square problem using $\mathbf{u}(t)$ ⁷.

Theorem 2 (informal). *Given $A \in \mathbb{R}^{m \times n}$, $\mathbf{b} \in \mathbb{R}^m$, and $\epsilon > 0$. Let $\mathbf{x}(t)$ be the firing rate of the above stochastic SNN with proper parameter setting. When $t = \Theta(\frac{\kappa^2 n \cdot \|\mathbf{x}^{\ell_2}\|_2 \ln(\frac{\kappa n}{\epsilon \delta})}{\epsilon})$, $\mathbf{x}(t)$ is a probabilistic (ϵ, δ) -approximate solution for the least square problem of (A, \mathbf{b}) where λ_{\max} is the largest eigenvalues of $A^\top A$, κ is the condition number of $A^\top A$ ⁸, and $\mathbf{x}^{\ell_2} = \arg \min_{\mathbf{x}: A^\top A \mathbf{x} = A^\top \mathbf{b}} \|\mathbf{x}\|_2$ is the least square solution. Specifically, the timestep complexity of stochastic SNN to produce a probabilistic (ϵ, δ) -approximate solution is $T = O(\frac{\kappa^2 n \cdot \|\mathbf{x}^{\ell_2}\|_2 \ln(\frac{\kappa n}{\epsilon \delta})}{\epsilon})$.*

An interesting point in Theorem 2 to note is that we do not need to assume $A^\top A$ to have full rank, and hence the objective function $\|\mathbf{b} - A\mathbf{x}\|_2^2/2$ may not be strongly convex, which is usually assumed for stochastic gradient algorithms. The reason that we do not require $A^\top A$ to be full rank is that in the stochastic SNN dynamics, $\mathbf{u}(t)$ always lies in the range space of $A^\top A$. Thus, stochastic SNN implicitly executes the stochastic gradient algorithms in the range space of $A^\top A$, where the objective function $\|\mathbf{b} - A\mathbf{x}\|_2^2/2$ becomes strongly convex with respect to $\mathbf{u}(t)$.

Simple SNN as a primal-dual algorithm. We now revisit the simple SNN dynamics discussed above, and consider the situation where the linear system $A\mathbf{x} = \mathbf{b}$ is under-determined (as opposed to the over-determined situation for the least square problem). A natural question is to ask which solution does the firing rate of simple SNN converge to?

We observe (from simulations) that the firing rate always converges to the solution with the *smallest* ℓ_1 norm, which suggests that simple SNN solves the ℓ_1 minimization problem in the under-determined case. ℓ_1 minimization problem is a well-studied problem that arises in several contexts such as compressive sensing with a rich literature of algorithms and implementations [YSGM10].

Interesting, we observe that the simple SNN dynamics can be viewed as a *primal-dual* algorithm for solving the ℓ_1 minimization problem, which is, to the best of our knowledge, different from

⁷Stochastic SNN is also doing an approximate stochastic gradient descent with $\mathbf{x}(t)$. For the convenience of the presentation, here we only mention $\mathbf{u}(t)$.

⁸Please refer to Section 2 for formal definitions.

existing algorithms. Furthermore, our simulation result in Section 6.4 shows that simple SNN can solve certain random ℓ_1 minimization instances with comparable efficiency to the ℓ_1 -magic package [CR05b] especially for large instances (but with a relatively large error).⁹ It is intriguing to us that simple SNN may solve the well-studied ℓ_1 minimization problem with a new algorithm with comparable efficiency at least for certain nice instances.

Unfortunately, we do not know how to prove the convergence of the dynamics, and we view it as a very interesting open question. In Section 6, we present an in-depth discussion of the primal-dual algorithm and the challenges to analyze it. We also analyze a related dynamics, which can be thought of as a “smoothed” simple SNN dynamics with the spiking strength $\alpha \rightarrow 0$, and show that its “firing rate” converges to an optimal solution of the ℓ_1 minimization problem. We view it as a partial evidence that simple SNN may solve the ℓ_1 minimization problem as well.

In what follows, we briefly illustrate how to interpret the simple SNN dynamics as a primal-dual algorithm for the ℓ_1 minimization problem. We refer to Section 6 for detailed discussion. We first write down the ℓ_1 minimization problem and its dual.

$$\begin{array}{ll} \underset{\mathbf{x} \in \mathbb{R}^n}{\text{minimize}} & \|\mathbf{x}\|_1 \\ \text{subject to} & \mathbf{A}\mathbf{x} = \mathbf{b}. \end{array} \quad (4)$$

$$\begin{array}{ll} \underset{\mathbf{v} \in \mathbb{R}^m}{\text{maximize}} & \mathbf{b}^\top \mathbf{v} \\ \text{subject to} & \|A^\top \mathbf{v}\|_\infty \leq 1. \end{array} \quad (5)$$

Let us also recall the simple SNN dynamics and refer to it as the primal dynamics. Then, we will define a dual dynamics. To match the above programs, we set $\eta = 1$. For the primal dynamics, we have $t \in \mathbb{N}$,

$$\mathbf{u}(t+1) = \mathbf{u}(t) - \alpha \cdot A^\top A \cdot \mathbf{s}(t) + A^\top \mathbf{b} \cdot \Delta t. \quad (6)$$

We define a dual dynamics for $\mathbf{v}(t) \in \mathbb{R}^m$ satisfying $\mathbf{u}(t) = A^\top \mathbf{v}(t)$ as follows. For any $t \in \mathbb{N}$,

$$\mathbf{v}(t+1) = \mathbf{v}(t) - \alpha \cdot A\mathbf{s}(t) + \mathbf{b} \cdot \Delta t. \quad (7)$$

It can be shown that the primal and dual dynamics are in fact isomorphic to each other (since the primal vector $\mathbf{u}(t)$ always lies in the range space of $A^\top A$). Thus, we can switch between the primal and dual dynamics interchangeably.

Now we observe that the dual dynamics can be viewed as a variant of the gradient descent algorithm to solve the dual program. Indeed, without the spiking term, $\mathbf{v}(t)$ simply moves towards the gradient direction \mathbf{b} of the dual objection function. For the spike term $-\alpha \cdot A\mathbf{s}(t)$, note that $\mathbf{s}_i(t) \neq 0$ (i.e., neuron i fires) if and only if $|A_i^\top \mathbf{v}(t)| = |\mathbf{u}_i(t)| > 1$, which means $\mathbf{v}(t)$ is outside the feasible polytope of the dual program. Thus, one can view the role of the spike term as to push $\mathbf{v}(t)$ back to the feasible polytope, though this is different from the standard gradient descent algorithm that projects $\mathbf{v}(t)$ back to the feasible polytope.

Therefore, we can interpret the simple SNN dynamics as follows. The dynamics runs a gradient descent algorithm to solve the dual program. When the dual vector $\mathbf{v}(t)$ becomes infeasible, it triggers some spikes, which maintains the dual feasibility and update the primal solution (the firing rate). In Section 6, we argue that if $\mathbf{v}(t)$ is close to and move around the optimal point \mathbf{v}^* of the dual program, then the induced firing rate $\mathbf{x}(t)$ will indeed converge to an optimal solution of the primal program. We formulate the following conjecture based on our simulation result and our analysis of the related ideal dynamics (see Section 6.2).

⁹The random instances we consider are instances with a random matrix $A \in \mathbb{R}^{m \times n}$ for $m = n/4$ and a sparse optimal solution x^{ℓ_1} with $k = O(1)$ non-zero coordinates. Such instances are considered in the compressive sensing context.

Conjecture 1. *Given $A \in \mathbb{R}^{m \times n}$ and $\mathbf{b} \in \mathbb{R}^m$ such that there exists a solution for $A\mathbf{x} = \mathbf{b}$. Let $\mathbf{x}(t)$ be the firing rate of a simple SNN dynamics with proper parameter setting, for every $t \in \mathbb{N}$, $\mathbf{x}(t)$ is a $(\epsilon(t), \gamma(t))$ -approximate solution for the ℓ_1 minimization problem of (A, \mathbf{b}) , where $\epsilon(t), \gamma(t)$ converge to 0 as t goes to infinity.*

1.2 Perspective and Discussion

In this work, we answer Question 1 and Question 2 by showing that SNN with simple spiking rules can implement non-trivial stochastic gradient descent and primal-dual algorithms for solving least square and ℓ_1 minimization problems. Previous works of Shapero et al. [SZHR14] and Tang et al. [TLD17] also showed that SNN can be configured to implement LCA and solve the Lasso problem. These two results reveal the rich power of the SNN dynamics as natural algorithms for optimization problems, and we may only scratch the surface of its power. In our eyes, it is intriguing to further investigate the algorithmic power of SNN. In the following, we discuss three future research directions.

First, push further the analysis of simple SNN and stochastic SNN. In this work, we only partially answer Question 3 by showing the convergence of the parallel time complexity for least square problem. The main question left open in this work is to show that simple SNN solves the ℓ_1 minimization problem. Also, there is no non-trivial spike complexity bound being proved even for the least square problem. On the other hand, our timestep complexity bounds may not be tight. In particular, the simulation results suggest that the complexity of simple SNN may depend on the sparsity of the solution. It is interesting to understand its exact complexity. Finally, given the parallel nature of SNN algorithms, it is conceivable that SNN algorithms may achieve asymptotically better parallel complexity for certain optimization problem (e.g., the ℓ_1 minimization problem) than the existing algorithms. In particular, it seems plausible that SNN may solve the ℓ_1 minimization problem with similar timestep complexity $O(n\kappa/\epsilon)$ as solving the least square problem (as suggested by our analysis for the “smoothed” version and is compatible with our experiment). Thus, SNN can potentially lead to a new algorithm for the ℓ_1 minimization problem with faster parallel runtime in the dependency on n .

Second, investigate the potential of SNN dynamics as natural algorithms. The question is two-fold: (i) What algorithms can SNN implement? (ii) What computational problems can SNN solve? It seems that SNN is good at dealing with sparsity. Could it be helpful in related computational tasks such as fast Fourier transform (FFT) or sparse matrix-vector multiplication? It is interesting to identify optimization problems and class of instances where SNN algorithm can outperform other algorithms.

Third, explore the practical advantage of SNN dynamics as natural algorithms. The potential practical time efficiency, energy efficiency, and simplicity for hardware implementation have been suggested in several works [MMI15, BIP15, BPLG16]. Our simulation results also suggest potential advantage of simple SNN for random instances of the ℓ_1 minimization problem. It would be exciting to see SNN’s performance on practical applications such as compressed sensing, Lasso, and etc.

Finally, we remark that our work focuses on the algorithmic power of the SNN model, but we do not consider how the parameters can be obtained/learned in a natural SNN system. The learning aspect is of course an intriguing research direction, and we hope that our study of algorithmic aspect can shed some lights for the learning aspect.

1.3 Organization

In Section 2 we give notations and define two optimization problems. Section 3 builds up the framework of SNN algorithms. Section 4, Section 5, and Section 6 discuss simple SNN for least square, stochastic SNN for least square, and simple SNN for ℓ_1 minimization respectively.

2 Preliminaries

In Section 2.1, we build up some notations for the rest of the paper. In Section 2.2, we define two optimization problems and the corresponding convergence guarantees.

2.1 Notations

Let us begin with some notations. Let $\mathbf{x}, \mathbf{y} \in \mathbb{R}^n$ be two vectors. $|\mathbf{x}| \in \mathbb{R}^n$ denotes the entry-wise absolute value of \mathbf{x} , *i.e.*, $|\mathbf{x}|_i = |\mathbf{x}_i|$ for any $i \in [n]$. $\mathbf{x} \preceq \mathbf{y}$ refers to entry-wise comparison, *i.e.*, $\mathbf{x}_i \leq \mathbf{y}_i \forall i \in [n]$.

Let A be an $m \times n$ real matrix. For any $i \in [n]$, denote the i th column of A as A_i and its negation to be A_{-i} , *i.e.*, $A_{-i} = -A_i$. When A is a square matrix, we define the A -norm of a vector $\mathbf{x} \in \mathbb{R}^n$ to be $\|\mathbf{x}\|_A := \sqrt{\mathbf{x}^\top A \mathbf{x}}$. Let A^\dagger to be the pseudo-inverse of A . Define the maximum eigenvalue of a square matrix A as $\lambda_{\max}(A) := \max_{\mathbf{x} \in \mathbb{R}^n} \|\mathbf{x}\|_A / \|\mathbf{x}\|_2$, the minimum non-zero eigenvalue of A to be $\lambda_{\min}(A) := 1 / (\max_{\mathbf{x} \in \mathbb{R}^n} \|\mathbf{x}\|_{A^\dagger} / \|\mathbf{x}\|_2)$, and the condition number of A to be $\kappa(A) := \lambda_{\max}(A) / \lambda_{\min}(A)$. If we do not specify, the following λ_{\max} , λ_{\min} , and κ are the eigenvalues and condition number of $A^\top A$. For any $\mathbf{b} \in \mathbb{R}^m$, we denote \mathbf{b}_A to be the projection of \mathbf{b} on the range space of A . Finally, we denote $\mathbf{x}^{\ell_2} = \arg \min_{\mathbf{x}: A\mathbf{x}=\mathbf{b}_A} \|\mathbf{x}\|_2$ as the least square solution.

We say a vector function $\mathbf{F} : \mathbb{R}^n \rightarrow \mathbb{R}^n$ is *coordinate-wise* if there exists a function $F : \mathbb{R} \rightarrow \mathbb{R}$ such that for any $i \in [n]$ and $\mathbf{x} \in \mathbb{R}^n$, $(\mathbf{F}(\mathbf{x}))_i = F(\mathbf{x}_i)$.

2.2 Optimization problems

In this subsection, we are going to introduce two optimization problems: *least square* and *ℓ_1 minimization*. We will formally define each problem and the corresponding error measure.

2.2.1 Least square

Problem 1 (Least square). *Let $m, n \in \mathbb{N}$. Given $A \in \mathbb{R}^{m \times n}$ and vector $\mathbf{b} \in \mathbb{R}^m$, find $\mathbf{x} \in \mathbb{R}^n$ that minimizes $\|\mathbf{b} - A\mathbf{x}\|_2^2/2$. Equivalently, find $\mathbf{x} \in \mathbb{R}^n$ that makes $\|\mathbf{b}_A - A\mathbf{x}\|_2 = 0$ where \mathbf{b}_A is the projection of \mathbf{b} on the range space of A .*

Remark 1. *Let \mathbf{x}^* be an arbitrary solution of $A\mathbf{x} = \mathbf{b}$. In the context of optimization and algorithm design, it is more standard to use $\|\mathbf{x}^* - \mathbf{x}\|_{A^\top A}$ as the error measure for least square problem. However, since we consider the case where $A\mathbf{x} = \mathbf{b}$ having more than one solution, the definition of $\|\mathbf{x}^* - \mathbf{x}\|_{A^\top A}$ could be confusing since \mathbf{x}^* might not be unique. As a result, here we use $\|\mathbf{b}_A - A\mathbf{x}\|_2$ as our error measure. Nevertheless, note that $\|\mathbf{b}_A - A\mathbf{x}\|_2 = \|\mathbf{x}^* - \mathbf{x}\|_{A^\top A}$ and thus our definition is actually equivalent to the standard definition.*

The SNN algorithm might not solve the least square problem exactly and thus we define the following notions of solving least square problem *approximately*.

Definition 1 (ϵ -approximate solution for least square). Let $m, n \in \mathbb{N}$ and $\epsilon > 0$. Given $A \in \mathbb{R}^{m \times n}$ and $\mathbf{b} \in \mathbb{R}^m$. We say \mathbf{x} is a ϵ -approximate solution for the least square problem of (A, \mathbf{b}) if $\|\mathbf{b}_A - A\mathbf{x}\|_2 \leq \epsilon \|\mathbf{b}_A\|_2$.

Definition 2 (probabilistic (ϵ, δ) -approximate solution for least square). Let $m, n \in \mathbb{N}$, $\epsilon > 0$, and $\delta \in (0, 1)$. Given $A \in \mathbb{R}^{m \times n}$ and $\mathbf{b} \in \mathbb{R}^m$. We say $\mathbf{x}(t)$ is a probabilistic (ϵ, δ) -approximate solution for the least square problem of (A, \mathbf{b}) if with probability at least $1 - \delta$, $\mathbf{x}(t)$ is an ϵ -approximate solution for the least square problem of (A, \mathbf{b}) .

When matrix A is under-determined, there could be infinitely many solutions for the least square problem. We are interested in two specific solutions: the ℓ_1 minimum solution and the ℓ_2 minimum solution. Define $\mathbf{x}^{\ell_1} = \arg \min_{\mathbf{x}: A\mathbf{x}=\mathbf{b}_A} \|\mathbf{x}\|_1$ and $\mathbf{x}^{\ell_2} := \arg \min_{\mathbf{x}: A\mathbf{x}=\mathbf{b}_A} \|\mathbf{x}\|_2$ respectively. Note that \mathbf{x}^{ℓ_2} is the unique solution in the range space of $A^T A$ because the range space is orthogonal to the null space.

2.2.2 ℓ_1 minimization

Problem 2 (ℓ_1 minimization). Let $m, n \in \mathbb{N}$. Given $A \in \mathbb{R}^{m \times n}$ and $\mathbf{b} \in \mathbb{R}^m$ such that there exists a solution for $A\mathbf{x} = \mathbf{b}$. The goal of ℓ_1 minimization is to solve the following optimization problem.

$$\begin{aligned} & \underset{\mathbf{x} \in \mathbb{R}^n}{\text{minimize}} && \|\mathbf{x}\|_1 \\ & \text{subject to} && A\mathbf{x} = \mathbf{b}. \end{aligned} \tag{8}$$

Similarly, we do not aspire for SNN algorithm to be able to solve the ℓ_1 minimization exactly. Thus, we define the notion of solving ℓ_1 minimization problem *approximately* as follows.

Definition 3 ((ϵ, γ) -approximate solution for ℓ_1 minimization). Let $m, n \in \mathbb{N}$ and $\epsilon, \gamma > 0$. Given $A \in \mathbb{R}^{m \times n}$ and $\mathbf{b} \in \mathbb{R}^m$. Let \mathbf{OPT}^{ℓ_1} denote the optimal value of the ℓ_1 minimization problem of (A, \mathbf{b}) . We say $\mathbf{x} \in \mathbb{R}^n$ is an (ϵ, γ) -approximate solution of the ℓ_1 minimization problem of (A, \mathbf{b}) if $\|\mathbf{b} - A\mathbf{x}\|_2 \leq \epsilon \cdot \|\mathbf{b}\|_2$ and $\|\mathbf{x}\|_1 - \mathbf{OPT}^{\ell_1} \leq \gamma \cdot \mathbf{OPT}^{\ell_1}$.

3 SNN algorithms

In this section, we focus on the modeling aspect of SNN. We start by formulating a general discrete-time SNN model in Section 3.1 that captures the fundamental properties of SNN. Next, to justify the definition of our SNN model, we compare it with other SNN models in Section 3.2.

3.1 A Discrete-time SNN Model

In this section, we formulate a discrete-time analogue of the integrate-and-fire SNN model. We note that our goal is not to model the actual spiking neural networks studied in neuroscience, but instead, we aim for defining a simplest abstract model that captures the SNN algorithms we consider. We believe that it better highlights the algorithmic power of the SNN dynamics. To put our model in context, we discuss the relation between our model and the other integrate-and-fire models in literature.

A discrete-time SNN model. A (discrete-time) SNN is a dynamical system among n neurons indexed by $1, 2, \dots, n$, each of which is associated with a time-varying *potential*¹⁰ value. The dynamics proceeds in timestep $t \in \mathbb{N}$, where each timestep corresponds to an elapsed time Δt , where $\Delta t > 0$ is the *timestep size* parameter. For each $i \in [n] := \{1, 2, \dots, n\}$ and $t \in \mathbb{N}$, $\mathbf{u}_i(t) \in \mathbb{R}$ denotes the potential of neuron i at timestep t and $\mathbf{u}(t)$ denotes the vector of the neurons' potential at timestep t . We assume $\mathbf{u}_i(1) = 0$ for all $i \in [n]$. The dynamics of $\mathbf{u}(t)$ is governed by two factors: *external charging*¹¹ and *spikes*.

- **External charging** A neuron may receive certain external charging (could be negative) adding to its potential. Here we only consider constant external charging described by a constant vector $\mathbf{I} \in \mathbb{R}^n$, where each neuron i is charged by $\mathbf{I}_i \in \mathbb{R}$ per unit of time (i.e., charged by $\mathbf{I}_i \cdot \Delta t$ per timestep).
- **Spike** At each timestep, each neuron may fire a *spike* signal to other neurons. We consider (non-standard) *two-sided* spikes, where a neuron may fire positive or negative spike (denoted by $+1, -1$, respectively). The spikes are determined by applying a spiking rule function $R : \mathbb{R} \rightarrow \{-1, 0, 1\}$ (possibly randomized) to each neuron's potential (before receiving the external charge). Namely, $R(\mathbf{u}_i(t))$ determines whether neuron i fires a spike at timestep t , where $R(\mathbf{u}_i(t)) = 1$ (resp., $R(\mathbf{u}_i(t)) = -1$) means neuron i fires a positive (resp., negative) spike, and $R(\mathbf{u}_i(t)) = 0$ means no spike. For example, in the threshold spiking rule, a neuron fires if its potential exceeds a certain threshold parameter η (specifically, $R(u) = 1$ if $u \geq \eta$, $R(u) = -1$ if $u \leq -\eta$ and $R(u) = 0$ otherwise). For convenience, We use $\mathbf{R} : \mathbb{R}^n \rightarrow \{-1, 0, 1\}^n$ to denote a function that applies R to each coordinate $i \in [n]$, and $\mathbf{s}(t) := \mathbf{R}(\mathbf{u}(t))$ to denote the spike vector at timestep t .

When a neuron fires a spike signal to other neurons, it affects their potentials. The effect of spikes is described by the *connectivity matrix* $C \in \mathbb{R}^{n \times n}$ and the spiking strength parameter $\alpha > 0$. Specifically, when neuron i fires a positive (resp., negative) spike, the potential of neuron j will decrease (resp., increase) by $\alpha \cdot C_{ij}$ for any $j \in [n]$. In particular, the potential of neuron i itself decreases (resp., increases) by $\alpha \cdot C_{ii}$. Note that a positive (resp., negative) C_{ij} means that the spike of neuron i causes an inhibition effect (resp., exhibition effect) to neuron j .

To summarize, a SNN dynamics is specified by the external charging vector \mathbf{I} , the connectivity matrix C , the spiking rule function R , the spiking strength α , and the timestep size Δt , and determined by the following equation.

$$\mathbf{u}(t + 1) = \mathbf{u}(t) - C\mathbf{s}(t) + \mathbf{I} \cdot \Delta t, \quad (9)$$

where $\mathbf{s}(t) = \mathbf{R}(\mathbf{u}(t))$. An important statistic of the dynamics is the neurons' *firing rate*, which is the average number of spikes fired by each neuron. For each neuron i , we define its firing rate at timestep t to be $\mathbf{x}_i(t) := \left(\sum_{1 \leq s \leq t} \mathbf{s}_i(s) \right) / (t \cdot \Delta t)$.

Complexity measures for SNN algorithms A SNN algorithm basically contains three steps: First, configure a SNN based on the given input(s). Next, simulate the SNN for a sufficient number

¹⁰Sometimes being referred to *membrane potential*, *voltage* or *state variable*.

¹¹Sometimes being referred to *input signal* or *input current*.

of timesteps. Finally, output a statistics of the SNN (we focus on outputting the firing rate $\mathbf{x}(t)$ in this paper). Our goal is to understand the power and complexity of SNN algorithms for solving optimization problems. It has the advantage of simplicity, and its distributed nature makes it easy to be parallelized or to be implemented as a distributed algorithm.

To analyze the complexity of a SNN algorithm, two natural complexity measures are the number of timesteps (referred to timestep complexity and denoted as T) and the total number of spikes (referred to spike complexity and denoted as S). Formally, define $S = \sum_{1 \leq s \leq T} \sum_{i \in [n]} |\mathbf{s}_i(s)|$.

Connection to parallel and total time complexity Observe that when simulating a SNN algorithm, the time complexity would be $O(n \cdot (T + S))$ where the first term is due to the updates of external charging in each iteration and the second term is due to the updates whenever there is a spike. Note that the parallel time complexity would be $O(T + S)$ since the updates of both external charging and spikes can be parallelized. Furthermore, $n \cdot T$ is a trivial upper bound for S since this is the number of spikes when every neuron fire at every timestep.

3.2 Compare with other SNN models

Before continuing, we discuss several aspects where our model differs from existing integrate-and-fire models to put our model in context.

Discrete-time versus continuous-time. In literature, SNN dynamics are typically modeled in the continuous-time setting to describe the dynamics of integrate-and-fire neural networks. While we defined a discrete-time model, one can consider a continuous-time analogue by taking $\Delta t \rightarrow 0$. Specifically, the corresponding continuous-time model can be described by the following differential equation.

$$\frac{d}{dt} \mathbf{u}(t) = -C\mathbf{s}(t) + \mathbf{I}, \quad (10)$$

where $\mathbf{s}(t)$ records each spike by a delta function $\delta(\cdot)$. Namely, for every $i \in [n]$, let $\{t_{ik}\}_k$ be the timestep neuron i fires a spike, we have $\mathbf{s}_i(t) = \sum_k \delta(t - t_{ik}) \cdot R(\mathbf{u}_i(t_{ik}))$.

We choose to work with the discrete-time model since our goal is to explore the algorithmic aspects and computational complexity of SNN, and the discrete-time model provides concrete complexity measures (e.g., number of timesteps and spikes). Working with the discrete-time model also makes the analysis cleaner. In contrast, it is less clear how to measure the complexity of a continuous-time SNN model. Also, we still need to consider discretized timestep when we want to simulate a continuous-time SNN. Nevertheless, since the continuous-time model captures the actual neuron dynamics better, we believe it is interesting to consider the complexity of the continuous-time model.

We mention that in some continuous-time models (e.g., [PMB12]), the effect of spikes is not instantaneous (as modeled by the delta function above). Instead, the delta function is replaced with an exponentially decrease function, say $e^{-c \cdot (t - t_{ik})}$ for some $c > 0$. The distinction is not captured in the discrete-time model, but the difference seems inconsequential for the computational power of SNN.

One-sided spikes versus two-sided spikes. Another major difference in our model is that we consider two-sided spiking rule where a neuron can fire either positive or negative spikes. In contrast, SNN models in the literature (e.g., [Lap07, Adr26, HH52, Ste65, PMB12]) consider neurons with one-sided spiking rule to capture actual neurons. Namely, each neuron only fires a single-type spike when, e.g., its potential exceeds a certain threshold.

We choose to consider the (non-standard) two-sided spiking rule since it facilitates our study on the algorithmic aspect of SNN. In particular, it helps to introduce symmetry and configure SNN algorithms for optimization problems with cleaner analyses.

We note that two-sided spiking rules are not stronger in the sense that an SNN with two-sided spiking rule can be simulated by an SNN with one-sided spiking rule with a double number of neurons. Roughly speaking, this can be done by duplicating the neurons and let each copy to simulate positive and negative spikes separately. The connectivity matrix C and external charging vector \mathbf{I} are correspondingly modified to be

$$\bar{C} = \begin{pmatrix} C & -C \\ -C & C \end{pmatrix} \text{ and } \bar{\mathbf{I}} = \begin{pmatrix} \mathbf{I} \\ -\mathbf{I} \end{pmatrix}.$$

On the other hand, we do not know if the two-sided SNN model can simulate the one-sided SNN model, so the two-sided model may in fact be more restrictive.

Potential-dependent charging rules. Finally, note that in our model, we only consider constant external charging. We mention that several SNN models consider charging rules that depend on the current potential value of each neuron. For example, [BDM13] considers the “leaky integrate-and-fire neurons” where an additional $-\tau \mathbf{u}(t) \cdot \Delta t$ term on the right hand side of (9) for some $\tau > 0$. Another SNN model considered in [TLD17] has a *signed drift* where there is an additional constant term on the right hand side of (9) such that the sign of this constant drift depends on the sign of current potential value. Our SNN algorithms do not need the generality of potential-dependent charging rules, but it is interesting to see if such generality adds certain power to the SNN algorithms.

4 A simple SNN algorithm for least square

In this section, we investigate SNN with a simple threshold spiking rule (which we refer to as *simple SNN*), and show that when configured properly, such simple SNN dynamics can solve the least square problem. Specifically, we consider a threshold rule $R = R_\eta$ for some threshold parameter $\eta > 0$, defined as follows.

$$R_\eta(u) = \begin{cases} 1 & , u > \eta \\ 0 & , -\eta \leq u \leq \eta \\ -1 & , u < -\eta. \end{cases} \quad (11)$$

In other words, each neuron fires a positive (resp., negative) spike at timestep t if its potential (at beginning of the timestep) exceeds η (resp., goes below $-\eta$). Note that for simple SNN, by scaling the parameters,¹² we can assume w.l.o.g., that the spiking strength $\alpha = 1$. Thus, the dynamics can be described by the following equation. For any $t \in \mathbb{N}$,

$$\mathbf{u}(t+1) = \mathbf{u}(t) - C\mathbf{s}(t) + \mathbf{I} \cdot \Delta t, \quad (12)$$

¹²For any triple $(\alpha, \eta, \Delta t)$, when scaling to $(1, \eta/\alpha, \Delta t/\alpha)$, the behavior of the simple SNN remains the same.

where $\mathbf{s}(t) = \mathbf{R}_\eta(\mathbf{u}(t))$. We note that threshold spiking rule is a common ingredient in SNN dynamics and simple SNN is arguably the simplest SNN dynamics one may consider.

We start with a few simple observations to understand the dynamics of simple SNN. First note that the diagonal entries of the connectivity matrix should be positive, i.e., $C_{ii} > 0$, since otherwise, a neuron will continue to fire spikes and its potential will diverge to infinity. Also, if C is non-PSD, the potential value of some neurons might diverge. For instance, consider

$$C = \begin{pmatrix} 1 & 1 & -0.5 \\ 1 & 1 & -1 \\ -0.5 & -1 & 2 \end{pmatrix} \text{ and } \mathbf{I} = \begin{pmatrix} 1 \\ -1 \\ 0 \end{pmatrix}.$$

Note that the first neuron will move to the positive side while the second neuron will move to the negative side. One can see that the effects of the positive spike from neuron 1 and the effect of the negative pike from neuron 2 will cancel out with each other. Namely, once the two neuron leave the threshold simultaneously, the spikes will not help them going back to the non-spiking region. They will keep moving outward due to the external charging and thus diverge.

In addition to the property of the connectivity matrix C , if the parameters are not set properly, the potential value may also diverge to infinity. For example, consider the case where Δt is too large such that the external charging received by a neuron is greater than the inhibition of its own spike. In this example, the potential of a neuron can grow infinitely large.

Nevertheless, as we show below, if the parameters are properly chosen, then the neurons' potential will remain bounded. Furthermore, when properly configured, the firing rate will converge to an optimal solution of a given least square problem instance.

Simple SNN solves the least square problem. Recall that given a matrix $A \in \mathbb{R}^{m \times n}$ and a vector $\mathbf{b} \in \mathbb{R}^m$, the goal of the least square problem is to find $\mathbf{x} \in \mathbb{R}^n$ that minimizes $\|\mathbf{b} - A\mathbf{x}\|_2$. We configure an SNN algorithm for the least square problem: Given the instance (A, \mathbf{b}) , we simply configure a SNN dynamics of n neurons with connectivity matrix $C = A^\top A$, external charging vector $\mathbf{I} = A^\top \mathbf{b}$, and the initial potential vector $\mathbf{u}(1) = \mathbf{0}$. For the parameters, we require the threshold $\eta \geq \lambda_{\max}$ and the timestep size $\Delta t \leq \frac{\sqrt{\lambda_{\min}}}{24\sqrt{n} \cdot \|\mathbf{b}_A\|_2}$, where λ_{\min} and λ_{\max} are the minimal and maximal eigenvalues of $A^\top A$. The following theorem states that the residual error $\|\mathbf{b}_A - A\mathbf{x}(t)\|_2$ converges to zero.

Theorem 3. *Given $A \in \mathbb{R}^{m \times n}$, $\mathbf{b} \in \mathbb{R}^m$, and $\epsilon > 0$. Let $\mathbf{x}(t)$ be the firing rate of a simple SNN with $C = A^\top A$, $\mathbf{I} = A^\top \mathbf{b}$, $\alpha = 1$, $\eta \geq \lambda_{\max}$, and $\Delta t < \frac{\sqrt{\lambda_{\min}}}{24\sqrt{n} \cdot \|\mathbf{b}_A\|_2}$. When $t \geq \frac{48\kappa n}{\epsilon}$, $\mathbf{x}(t)$ is an ϵ -approximation solution to the least square problem of (A, \mathbf{b}) . In particular, if we set $\eta = \lambda_{\max}$ and $\Delta t = \frac{\sqrt{\lambda_{\min}}}{24\sqrt{n} \cdot \|\mathbf{b}_A\|_2}$, the timestep complexity of the simple SNN to produce ϵ -approximate solution is $T = O(\frac{\kappa n}{\epsilon})$.*

To the best of our knowledge, this is the first result proving an explicit complexity bound for SNN dynamics as an algorithm for solving optimization problems. In contrast, previous results [TLD17] with a slightly different setting only formally established convergence results without explicit complexity bounds. On the other hand, note that here we need the information of λ_{\max} and λ_{\min} to configure the SNN, so it is only applicable when a good estimation of the parameters are known. Also, our theorem only bounds the timestep complexity T but not the spike complexity S . While one can bound the spike complexity by $n \cdot T$ since each neuron only fires at most one

spike in one timestep, the bound seems far from tight. It is an interesting question to analyze the spike complexity of the simple SNN algorithm.

Before proving the theorem, we first give some intuition about why should the firing rate converge to an optimal least square solution. An important fact here is that the neurons' potential $\mathbf{u}(t)$ will remain bounded (specifically, we will show that the $(A^\top A)^\dagger$ -norm of $\mathbf{u}(t)$ is bounded). Now, recall that the potential is affected by the constant external charging $\mathbf{I} \cdot \Delta t = A^\top \mathbf{b} \cdot \Delta t$ and the spike $-A^\top A \cdot \mathbf{s}$. Intuitively, for the potential to remain bounded, the constant external charging needs to be balanced by the effect of the spikes over time. Thus, in the limit, we should expect that $A^\top A \cdot \mathbf{x} \approx A^\top \mathbf{b}$, namely, the average effect of the spike should roughly be the external charging for one unit of time. Note that as $A^\top \mathbf{b} = A^\top \mathbf{b}_A$ and \mathbf{b}_A lies in the range space of A , this implies that $A\mathbf{x} \approx \mathbf{b}_A$. In the following, we start with a lemma about the properties of matrix norm and then prove the boundedness of $\mathbf{u}(t)$. Finally, we use the ‘‘potential conservation argument’’ to prove Theorem 3.

Lemma 1. *Let $A \in \mathbb{R}^{m \times n}$ and $\mathbf{b} \in \mathbb{R}^n$. We have*

1. For any $\mathbf{x} \in \mathbb{R}^n$, $\|\mathbf{x}\|_{A^\top A} = \|\mathbf{A}\mathbf{x}\|_2 = \|A^\top \mathbf{A}\mathbf{x}\|_{(A^\top A)^\dagger}$.

2. $\|A^\top \mathbf{b}\|_{(A^\top A)^\dagger} = \|\mathbf{b}_A\|_2$.

Proof. See Appendix 7.1 ■

Lemma 2. *For any time $t \in \mathbb{N}$. When the threshold $\eta \geq \lambda_{\max}$ and the discretized step $\Delta t < \frac{\sqrt{\lambda_{\min}}}{24\sqrt{n} \cdot \|\mathbf{b}_A\|_2}$, we have $\|\mathbf{u}(t)\|_{(A^\top A)^\dagger} \leq 2\sqrt{\kappa\eta n}$.*

Proof. The lemma can be proved with induction and some properties of the dynamics of SNN. See Appendix 7.2 for details. ■

We now prove Theorem 3 using Lemma 2.

Proof of Theorem 3: The proof consists of two steps. First, using the dynamics of $\mathbf{u}(t)$ to derive a connection between $\mathbf{u}(t)$ and the residual error of the least square problem. Second, use Lemma 2 to help upper bounding the residual error.

Let's start with telescoping (19) from time 1 to time t ,

$$\sum_{s=1}^t \mathbf{u}(s+1) = \sum_{s=1}^t \mathbf{u}(s) - A^\top \mathbf{A}\mathbf{s}(s) + A^\top \mathbf{b}\Delta t \tag{13}$$

$$= \left(\sum_{s=1}^t \mathbf{u}(s) \right) - t \cdot \Delta t \cdot \left(A^\top \mathbf{A}\mathbf{x}(t) - A^\top \mathbf{b} \right). \tag{14}$$

Subtract $\sum_{s=1}^t \mathbf{u}(s)$ on both sides and divide with $t \cdot \Delta t$, we have an elegant connection between the firing rate and the potential vector.

$$\frac{\mathbf{u}(t+1) - \mathbf{u}(1)}{t \cdot \Delta t} = A^\top \mathbf{b} - A^\top \mathbf{A}\mathbf{x}(t). \tag{15}$$

Note that the right-hand side of (15) is A^\top multiplying the residual error $\mathbf{b} - \mathbf{A}\mathbf{x}(t)$. To get rid of the A^\top term, we apply the $(A^\top A)^\dagger$ -norm on the both sides of (15). By Lemma 1 and the fact that \mathbf{b}_A is the projection of \mathbf{b} on the range space of A , we have

$$\frac{\|\mathbf{u}(t+1) - \mathbf{u}(1)\|_{(A^\top A)^\dagger}}{t \cdot \Delta t} = \|A^\top \mathbf{b} - A^\top A \mathbf{x}(t)\|_{(A^\top A)^\dagger} = \|\mathbf{b}_A - A \mathbf{x}(t)\|_2. \quad (16)$$

As a result, to upper bound the error $\|\mathbf{b}_A - A \mathbf{x}(t)\|_2$, it suffices to upper bound $\|\mathbf{u}(t+1) - \mathbf{u}(1)\|_{(A^\top A)^\dagger}$. Moreover, as we take $\mathbf{u}(1) = \mathbf{0}$, now we only need to show $\|\mathbf{u}(t+1)\|_{(A^\top A)^\dagger}$ is bounded by some ϵ multiplicative factor of $\|\mathbf{b}_A\|_2$. As we take $\Delta t \leq \frac{\sqrt{\lambda_{\min}}}{24\sqrt{n} \cdot \|\mathbf{b}_A\|_2}$ and $\eta \geq \lambda_{\max}$, Lemma 2 tell us that $\|\mathbf{u}(t+1)\|_{(A^\top A)^\dagger} \leq 2\sqrt{\kappa\eta n}$ for any $t \in \mathbb{N}$. Combine this upper bound for $\mathbf{u}(t+1)\|_{(A^\top A)^\dagger}$ with (16), we have

$$\|\mathbf{b}_A - A \mathbf{x}(t+1)\|_2 \leq \frac{\|\mathbf{u}(t+1)\|_{(A^\top A)^\dagger}}{t \cdot \Delta t} \leq \frac{2\epsilon\sqrt{\kappa\eta n} \cdot \|\mathbf{b}_A\|_2}{2\sqrt{\kappa\eta n}} = \epsilon \cdot \|\mathbf{b}_A\|_2. \quad (17)$$

■

5 A stochastic SNN algorithm for least square

In this section, we investigate SNN with a stochastic threshold spiking rule (which we refer to as *stochastic SNN*). We show that the stochastic SNN also solves the least square problem, but in a different way — the dynamics can be interpreted as a natural stochastic gradient descent algorithm.

Specifically, we consider the following *stochastic threshold spiking rule* $R_\eta^{\text{stochastic}} : \mathbb{R} \rightarrow \{-1, 0, 1\}$, for some threshold parameter $\eta > 0$, defined as follows.

$$R_\eta^{\text{stochastic}}(u) = \begin{cases} \text{sgn}(u) & , \text{ with probability } \min\{\frac{|u|}{\eta}, 1\} \\ 0 & , \text{ with probability } 1 - \min\{\frac{|u|}{\eta}, 1\}. \end{cases} \quad (18)$$

In other words, the probability that a neuron fires is proportional to the magnitude of its potential and a neuron fires with certainty if the magnitude of its potential exceeds η . This can be viewed as a stochastic variant of the simple threshold spiking rule. The dynamics can be described as the following equation. For any $t \in \mathbb{N}$,

$$\mathbf{u}(t+1) = \mathbf{u}(t) - \alpha \cdot C \mathbf{s}(t) + \mathbf{I} \cdot \Delta t, \quad (19)$$

where $\mathbf{s}(t) = \mathbf{R}_\eta^{\text{stochastic}}$ and $\alpha > 0$ is the spiking strength.

Interestingly, by slightly changing the spiking rule, the stochastic SNN has a very different behavior as compared to the deterministic simple SNN. Intuitively, the potential vector $\mathbf{u}(t)$ of the stochastic SNN is performing a *stochastic gradient descent (SGD)* with respect to the objective function of the least square problem. Concretely, consider the objective function of the least square problem as follows.

$$f(\mathbf{u}) = \frac{1}{2} \|\mathbf{b} - A \mathbf{u}\|_2^2. \quad (20)$$

It is not hard to verify that f is convex with its gradient vector being

$$\nabla f(\mathbf{u}) = A^\top A \mathbf{u} - A^\top \mathbf{b}. \quad (21)$$

Now, rewrite the update rule of the stochastic SNN as follows. For any $t \in \mathbb{N}$

$$\mathbf{u}(t+1) = \mathbf{u}(t) - \mathbf{g}(t), \quad (22)$$

where $\mathbf{g}(t) = A^\top A \mathbf{s}(t) - A^\top \mathbf{b} \cdot \Delta t$. Observe that when conditioning on the event where $\|\mathbf{u}(t)\|_\infty \leq \eta$, the expectation of the update term $\mathbf{g}(t)$ is

$$\mathbb{E}[\mathbf{g}(t) \mid \|\mathbf{u}(t)\|_\infty \leq \eta] = \frac{A^\top A \mathbf{u}(t) - A^\top \mathbf{b}}{\eta} = \frac{\nabla f(\mathbf{u}(t))}{\eta}. \quad (23)$$

Namely, the expectation of the update term of $\mathbf{u}(t)$ is the gradient with respect to f . Once we can upper bound the length of $\mathbf{u}(t)$ with high probability, then by our conservation argument, we can get the convergence of the residual error.

The following theorem shows the convergence of the stochastic SNN.

Theorem 4. *Given $A \in \mathbb{R}^{m \times n}$, $\mathbf{b} \in \mathbb{R}^m$, and $\epsilon, \delta \in (0, 1)$. Let $\mathbf{x}(t) = \alpha \cdot \sum_{1 \leq s \leq t} \mathbf{s}(s)$ be the weighted firing rate of a stochastic SNN with $C = A^\top A$, $\mathbf{I} = A^\top \mathbf{b}$, $\eta = \Omega(\|\mathbf{x}^{\ell_2}\|_2)$, $\alpha = O(\frac{\eta}{\kappa \lambda_{\max} n \ln \frac{\kappa n}{\delta}})$, and $\Delta t = \alpha/\eta$. When we set $t = \Omega(\frac{\eta^2}{\epsilon \alpha \sqrt{\lambda_{\min}} \cdot \|\mathbf{b}_A\|_2})$, we have $\mathbf{x}(t)$ being a probabilistic (ϵ, δ) -approximate solution for the least square problem of (A, \mathbf{b}) . In particular, if we set $\eta = \Theta(\|\mathbf{x}^{\ell_2}\|_2)$ and $\alpha = \Theta(\frac{\eta}{\kappa \lambda_{\max} n \ln \frac{\kappa n}{\delta}})$, the timestep complexity of the stochastic SNN to produce probabilistic (ϵ, δ) -approximate solution is $T = O(\frac{\kappa^2 n \|\mathbf{x}^{\ell_2}\|_2 \ln(\frac{\kappa n}{\delta})}{\epsilon})$.*

Proof. See Appendix 8. ■

From the discussion above, the way the stochastic SNN performs stochastic gradient descent is not directly on the solution $\mathbf{x}(t)$. Instead, it is the potential vector $\mathbf{u}(t)$ updating in the direction of the gradient in expectation. Specifically, $\mathbf{u}(t)$ will stay close to \mathbf{x}^{ℓ_2} with high probability since $\mathbf{u}(t)$ lies in the range space of $A^\top A$ and \mathbf{x}^{ℓ_2} is the unique solution of $A\mathbf{x} = \mathbf{b}$ that lies in the range space of $A^\top A$. Note that by the definition of the spiking rule, when $\|\mathbf{u}(t)\|_\infty \leq \eta$, the expectation of $\mathbf{s}(t)$ is proportional to $\mathbf{u}(t)$, which will be close to \mathbf{x}^{ℓ_2} when t large enough with high probability. Intuitively, this observation hints that the firing rate of the stochastic SNN is converging to the ℓ_2 minimum solution while we believe that that of the simple SNN is converging to the ℓ_1 minimum solution. Although it is much more complicated to prove this connection, intuitively, one can see that by slightly modifying the spiking rule, SNN can perform different algorithmic ideas and solve different optimization problems.

6 The simple SNN as a primal-dual algorithm for ℓ_1 minimization

In this section, we revisit simple SNN. Our main finding is that interestingly, the dynamics of simple SNN can be viewed as a *primal-dual algorithm* for solving the ℓ_1 minimization problem. However, we are not able to formally analyze its convergence. Thus, after illustrating the primal-dual algorithm underlying the simple SNN dynamics, we discuss some evidence supporting its convergence as well as the challenges in the analysis.

To motivate the observation, recall that simple SNN solves the least square problem by configuring $C = A^\top A$ and $\mathbf{I} = A^\top \mathbf{b}$. When the linear system $A\mathbf{x} = \mathbf{b}$ is under-determined, a natural question is to ask which solution does the firing rate of simple SNN converge to? We observe (from simulation) that the firing rate always converges to the solution with the smallest ℓ_1 norm. Namely, simple SNN solves the following ℓ_1 minimization problem.

$$\begin{aligned} & \underset{\mathbf{x} \in \mathbb{R}^n}{\text{minimize}} && \|\mathbf{x}\|_1 \\ & \text{subject to} && A\mathbf{x} = \mathbf{b}. \end{aligned} \quad (24)$$

ℓ_1 minimization is a well-studied optimization problem in the context of finding the sparsest solution of a linear system. It has received much attention due to the success of compressive sensing [CDS01, C⁺06]. There are also practical packages for ℓ_1 minimization such as the ℓ_1 -magic [CR05b]. See [YSGM10] for a survey of several well-known algorithms for ℓ_1 minimization.

We now illustrate how does the dynamics of simple SNN implement a primal-dual algorithm for the ℓ_1 minimization problem. For this, let us first write down the dual program of the problem and discuss its basic properties.

$$\begin{aligned} & \underset{\mathbf{v} \in \mathbb{R}^m}{\text{maximize}} && \mathbf{b}^\top \mathbf{v} \\ & \text{subject to} && \|A^\top \mathbf{v}\|_\infty \leq 1. \end{aligned} \tag{25}$$

It will be convenient to introduce the following notation. For $i \in [n]$, let $A_{-i} = -A_i$. Let $[\pm n] = \{\pm 1, \pm 2, \dots, \pm n\}$. Thus, the feasible polytope of the dual program is defined by the constraints $A_j^\top \mathbf{v} \leq 1$ for $j \in [\pm n]$. For each $j \in [\pm n]$, we call the hyperplane $\{\mathbf{v} : A_j^\top \mathbf{v} = 1\}$ the *wall* W_j of the polytope. See Figure 1 and Figure 2 for example. Let \mathbf{v}^* denote the optimal solution of the dual program. It is easy to see that \mathbf{v}^* is the furthest corner of the polytope along the \mathbf{b} direction. Let $\Gamma^* = \{j \in [\pm n] : A_j^\top \mathbf{v}^* = 1\}$ be the index set of the walls that define the optimal corner \mathbf{v}^* . Let us call $\Gamma^* \subset [\pm n]$ the *active set* of \mathbf{v}^* . Note that one can connect \mathbf{v}^* to the optimal primal solution \mathbf{x}^{ℓ_1} via KKT conditions. By the complementary slackness condition, for any $i \in [n]$, if $i \in \Gamma$ (or $-i \in \Gamma$), then $\mathbf{x}_i^{\ell_1}$ should be positive (or negative). If both $i, -i \notin \Gamma$, then $\mathbf{x}_i^{\ell_1} = 0$. Thus \mathbf{x}^{ℓ_1} will be a solution of $A\mathbf{x} = \mathbf{b}$ that satisfies these conditions.

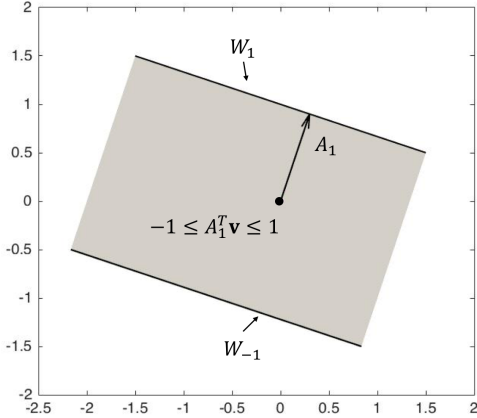


Figure 1: This is an example of single neuron. The characteristic vector is $A_1 = [\frac{1}{3} \ 1]^\top$. The positive wall of the neuron is W_1 , which is a line in this example. The inactive region is the gray area.

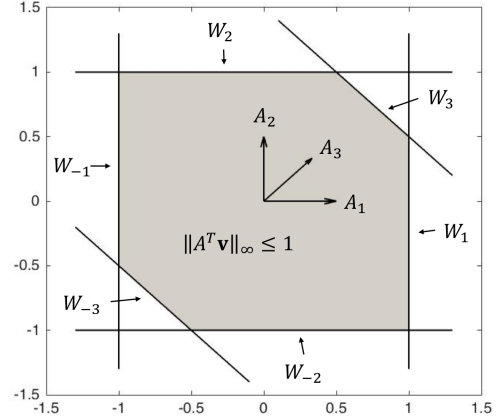


Figure 2: This is an example of three neurons. The characteristic vectors are $A_1 = [1 \ 0]^\top$, $A_2 = [0 \ 1]^\top$, and $A_3 = [\frac{2}{3} \ \frac{2}{3}]^\top$. The gray area, *i.e.*, the inactive polytope, is the region where no neuron will fire.

Now, the key observation is that by a linear transformation, the dynamics of simple SNN can be interpreted as a natural dynamics in the dual space to find optimal dual solution. We refer to it as a *dual SNN dynamics* and define it as follows.

6.1 A dual SNN dynamics.

We first recall the simple SNN dynamics. For convenience of the following discussion, we set the threshold parameter $\eta = 1$ (and make the spiking strength parameter α explicit). We refer to it as the primal dynamics here and recall it as follows. For any $t \in \mathbb{N}$,

$$\mathbf{u}(t+1) = \mathbf{u}(t) - \alpha \cdot A^\top A \cdot \mathbf{s}(t) + A^\top \mathbf{b} \cdot \Delta t. \quad (26)$$

We define a dual SNN dynamics for $\mathbf{v}(t) \in \mathbb{R}^m$ satisfying $\mathbf{u}(t) = A^\top \mathbf{v}(t)$ as follows. For any $t \in \mathbb{N}$,

$$\mathbf{v}(t+1) = \mathbf{v}(t) - \alpha \cdot A \mathbf{s}(t) + \mathbf{b} \cdot \Delta t. \quad (27)$$

Note that since the primal vector $\mathbf{u}(t)$ lies in the column space of A , we have $\mathbf{v}(t) = (A^\top)^\dagger \mathbf{u}(t)$, where $(A^\top)^\dagger$ is the pseudo-inverse of A^\top . Thus, the two dynamics are in fact *isomorphic* to each other. Therefore, in the following discussion, we may switch between the primal and the dual dynamics interchangeably.

Now let us understand the dual SNN dynamics. At each timestep, the external charging term $\mathbf{b} \cdot \Delta t$ is added to, and the spike term $A \mathbf{s}(t)$ subtracted from $\mathbf{v}(t)$. Note that \mathbf{b} is the gradient direction of the dual objective function. See Figure 3 for example. Thus, if there is no spike, $\mathbf{v}(t)$ simply takes one gradient step. For the spike term, recall that a neuron i fires if $|u_i(t)| > 1$ (recall that we set $\eta = 1$), which corresponds to $|A_i^\top \mathbf{v}(t)| > 1$ in the dual space. Thus, the spike term has the following nice geometric interpretation: if $\mathbf{v}(t)$ “hits” a wall W_j for some $j \in [\pm n]$, then neuron $|j|$ fires a spike and $\mathbf{v}(t)$ is “bounced back” by the wall W_j in the sense that $\mathbf{v}(t)$ is subtracted by $\alpha \cdot A_j$. See Figure 4 for example.

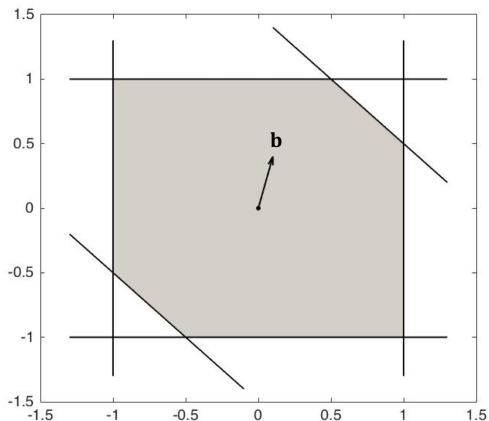


Figure 3: In this example, consider the same matrix A as in Figure 2 and $\mathbf{b} = [0.1 \ 0.4]^\top$.

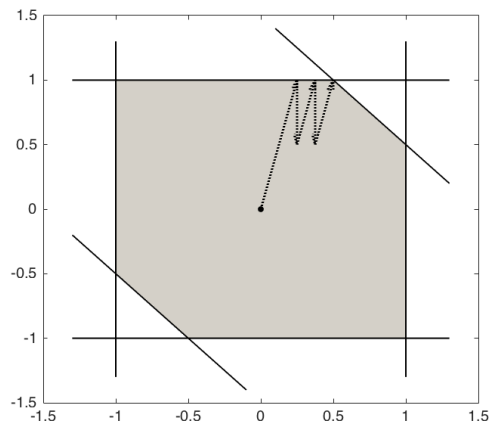


Figure 4: The execution of dual SNN on input in Figure 3.

Therefore, one can view the dual dynamics as doing a variant of the gradient descent algorithm to find the optimal dual solution, where to maintain the feasibility, the vector is not projected back to the feasible region as usual, but is “bounced back” by the wall W_j corresponding to the violated constraint $A_j^\top \mathbf{v} \leq 1$. An advantage of this variant is that the “bounce back” operation

is simply subtraction of $\alpha \cdot A_j$, which is significantly more efficient than projection back to the feasible region. On the other hand, note that the dynamics will not converge to the optimal dual solution \mathbf{v}^* . Intuitively, the best we can hope for is that $\mathbf{v}(t)$ will converge to bouncing around a small neighborhood region of \mathbf{v}^* (assuming the spiking strength α is sufficiently small).

The primal-dual connection. So far we saw that the dynamics of simple SNN can be viewed as a natural variant of the gradient descent algorithm for the dual program of the ℓ_1 -minimization problem. We now discuss some intuition about how the dual solution translates to the primal solution. For this, let us consider an ideal scenario where the dual vector $\mathbf{v}(t)$ is bounced around the optimal corner \mathbf{v}^* and only hits the walls W_j for $j \in \Gamma^*$, and ask what firing rate $\mathbf{x}(t)$ does it produce? Note that in this case, for each $i \in [n]$, neuron i fires positive (resp., negative) spikes if $i \in \Gamma$ (resp., $-i \in \Gamma$), and does not fire any spike if $i, -i \notin \Gamma$. This corresponds to $\mathbf{x}_i(t) \geq 0$ (resp., $\mathbf{x}_i(t) \leq 0$) if $i \in \Gamma$ (resp., $-i \in \Gamma$), and $\mathbf{x}_i(t) = 0$ otherwise. Recall the potential conservation argument, we expect that the effect of spike and external charging should balance each other. In other words, we expect that $A^\top A \mathbf{x}(t)$ converges to $A^\top \mathbf{b}$, which means $A \mathbf{x}(t)$ converges to \mathbf{b} ¹³ if the primal problem is feasible. Thus, $\mathbf{x}(t)$ will converge to a point that satisfies the KKT conditions, which is an optimal solution of the primal program.

Of course, the above discussion is informal and too idealized. In particular, note that the firing rate $\mathbf{x}(t)$ is not a feasible solution for the ℓ_1 minimization problem in general, and we only know that $A \mathbf{x}(t)$ will converge to \mathbf{b} . However, the above intuition suggests that simple SNN may find approximately feasible solutions that converge to an optimal solution for the ℓ_1 minimization problem. Specifically, let $\mathbf{OPT}^{\ell_1} = \|x^{\ell_1}\|_1$ denote the optimal value. We may hope that $\|\mathbf{b} - A \mathbf{x}(t)\|_2 \leq \varepsilon(t) \cdot \|\mathbf{b}\|_2$ and $\|x(t)\|_1 - \mathbf{OPT}^{\ell_1} \leq \gamma(t) \cdot \mathbf{OPT}^{\ell_1}$ for some vanishing $\varepsilon(t), \gamma(t) \rightarrow 0$, which is already interesting and useful for certain scenarios. In fact, as we discuss below in Section 6.4, our simulation result shows that simple SNN can solve certain random ℓ_1 minimization instances with comparable efficiency to the ℓ_1 -magic package [CR05b] especially for large instances.¹⁴

We are not able to prove such a result, but we formulate the following conjecture based on our simulation result and our analysis of a related dynamics (which we discuss below).

Conjecture 2. *Given $A \in \mathbb{R}^{m \times n}$ and $\mathbf{b} \in \mathbb{R}^m$ such that there exists a solution for $A \mathbf{x} = \mathbf{b}$. Let $\mathbf{x}(t)$ be the firing rate of a simple SNN with $C = A^\top A$, $\mathbf{I} = A^\top \mathbf{b}$, $\eta \geq \lambda_{\max}$, $\alpha = 1$, and $\Delta t = O\left(\frac{\sqrt{\lambda_{\min}}}{\sqrt{n} \cdot \|\mathbf{b}\|_2}\right)$. For any $t \in \mathbb{N}$, $\mathbf{x}(t)$ is a $(\varepsilon(t), \gamma(t))$ -approximate solution for the ℓ_1 minimization problem for (A, \mathbf{b}) , where $\varepsilon(t), \gamma(t) \in O(1/t)$ converge to 0 as t goes to infinity.*

In the following, we briefly discuss some challenges we encountered while proving the conjecture. Then we present some partial evidence we have to support the conjecture. Specifically, in Section 6.2, we consider a continuous-time dynamics (referred to as the *ideal SNN* dynamics) that in a sense corresponds to a “smoothed” simple SNN with $\alpha \rightarrow 0$. We show that the “firing rate” of this dynamics converges to an optimal solution of the ℓ_1 minimization problem. In addition to the ideal SNN, we report our simulation result of the simple SNN in Section 6.4, where we also present some “bad instances” that capture some difficulties for proving the conjecture.

¹³Because both $A \mathbf{x}(t)$ and \mathbf{b} lie in the range space of $A^\top A$.

¹⁴The random instances we consider are instances with a random matrix $A \in \mathbb{R}^{m \times n}$ for $m = n/4$ and a sparse optimal solution x^{ℓ_1} with $k = O(1)$ non-zero coordinates.

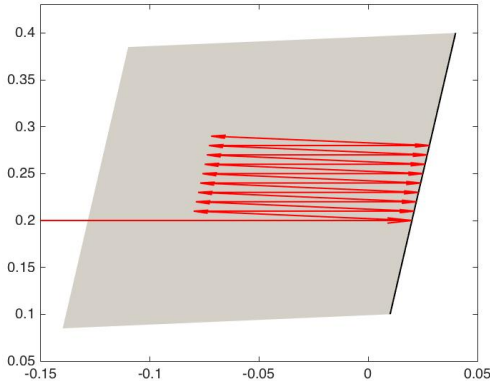


Figure 5: When \mathbf{b} is nearly orthogonal to a wall, the dual SNN will move very slowly.

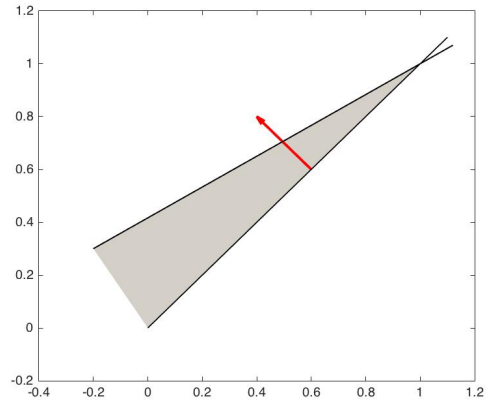


Figure 6: When the dual SNN goes to an acute corner, it might trigger a series of consecutive spikes.

Challenges in the analysis. We first observe that the dynamics of dual SNN may not find the optimal corner \mathbf{v}^* efficiently. The reason is that the gradient direction \mathbf{b} may be close to perpendicular to a wall W_j . In this case, the dual vector $\mathbf{v}(t)$ will keep hitting the wall and move very slowly along the wall. See Figure 5 for example. In fact, there is no explicit bound on the time it takes for $\mathbf{v}(t)$ to reach the optimal corner \mathbf{v}^* . Nevertheless, it can be shown that in this case, $\mathbf{b}^\top \mathbf{v}(t)$ is already close to the dual optimal value, and it seems plausible that the firing rate gives close-to-optimal primal objective value (though we do not know how to prove this). We note that this issue also comes up in the ideal SNN dynamics we consider in Section 6.2, where we can still show the convergence of the dynamics.

The main technical challenge is the “non-monotone behavior” of the dual SNN dynamics. A standard approach to analyze gradient-based algorithms is to argue that the algorithm makes non-negative progress towards the optimal solution. More precisely, one usually argues that there exists some appropriate distance measure d such that $d(\mathbf{v}(t), \mathbf{v}^*)$ monotonously decreases in a nontrivial way. In the dual SNN dynamics, however, the effect of spikes (i.e., bounced back by the walls) can be rather complicated. For example, when $\mathbf{v}(t)$ is near some acute corner, it can be bounced back and forth among multiple walls for multiple times. See Figure 6 for example. Thus, it seems unlikely that we can find a measure such that $\mathbf{v}(t)$ makes non-negative progress in every timestep. We note that this issue does not come up in the ideal SNN dynamics since there $\alpha \rightarrow 0$, which avoids the issue of bouncing back and forth among walls. A key element of the analysis is to show a monotone behavior of the ideal SNN dynamics.

6.2 An Ideal SNN Dynamics

In this section, we consider a continuous-time SNN dynamics in the dual space which we call the *ideal SNN dynamics*. Intuitively, the ideal SNN dynamics corresponds to a “smoothed” simple

SNN dynamics with the spiking strength $\alpha \rightarrow 0$ (and also $\Delta t \rightarrow 0$). Informally, imagine that when the dual vector $\mathbf{v}(t)$ hits a wall W_j , it will be bounced back by an infinitesimal amount, continue to move in \mathbf{b} direction, hit W_j immediately and bounced back by it again, and so on. This is effectively saying that the effect of \mathbf{b} will be partially canceled out by the effect of $-\alpha \cdot A_s(t)$ in a smooth way such that $\mathbf{v}(t)$ will move along the boundary of the polytope. It is tempting to define the direction $\mathbf{v}(t)$ is moving as the *projection* of \mathbf{b} onto the intersection of walls from $\Gamma(t)$. However, W_j can only contribute in the direction of $-A_j$, not the whole line spanned by A_j . That is, we should consider a more restricted projection that only allows a vector contributing in one sign instead of both. It turns out that the *conic projection* captures the property what we hope for. Formally, define the *conic projection* as follows.

Definition 4 (conic projection). *Let $A \in \mathbb{R}^{m \times n}$, $\Gamma \subseteq [\pm n]$, and $\mathbf{b} \in \mathbb{R}^m$. The conic projection of \mathbf{b} on the active set Γ of A is defined as follows.*

$$\mathbf{b}_{A,\Gamma} = \arg \min_{\mathbf{v} = \sum_{j \in \Gamma} a_j A_j, a_j \geq 0} \|\mathbf{b} - \mathbf{v}\|_2. \quad (28)$$

Moreover, the coefficient vector of the conic projection is defined as follows.

$$\mathbf{x}_{A,\mathbf{b},\Gamma} = \arg \min_{\mathbf{x} = (\mathbf{x}_1, \dots, \mathbf{x}_n): \text{if } i \in \Gamma, \mathbf{x}_i \geq 0; \text{ otherwise } \mathbf{x}_i = 0} \|\mathbf{b} - A\mathbf{x}\|_2. \quad (29)$$

Following the above discussion, for any $t \in \mathbb{N}$, let $\Gamma(t) := \{j \in [\pm n] \mid A_j^\top \mathbf{v}(t) = 1\}$ be the active set of dual SNN at time t such that $\mathbf{v}(t)$ is lying on the intersection of walls from $\Gamma(t)$ at time t . We define the ideal SNN to simulate the behavior of simple SNN with $\Delta t, \alpha \rightarrow 0$ in the extreme case where the spiking effect cancels \mathbf{b} in the perfect way, *i.e.*, minimizing $\|\mathbf{b} - \sum_{j \in \Gamma(t)} a_j A_j\|_2$ where $a_j \geq 0$. This is exactly the conic projection of \mathbf{b} on $\Gamma(t)$ of A . Specifically, $\mathbf{x}_{A,\mathbf{b},\Gamma(t)}$ is interpreted as the “local firing rate” of the ideal SNN dynamics at time t . To sum up, $\mathbf{b}_{A,\Gamma(t)} = \mathbf{b} - A\mathbf{x}_{A,\mathbf{b},\Gamma(t)}$ is the

Definition 5 (Ideal SNN dynamics). *Given an instance $A \in \mathbb{R}^{m \times n}$ and $\mathbf{b} \in \mathbb{R}^m$ of the ℓ_1 minimization problem, we define a continuous-time ideal SNN dynamics $\mathbf{v}^{ideal}(t)$ for $t \in \mathbb{R}^+$ with respect to the instance as follows. The initial condition is $\mathbf{v}^{ideal}(0) = 0$. For $t \geq 0$, the dynamics is defined by*

$$\frac{d}{dt} \mathbf{v}^{ideal}(t) = \mathbf{b} - \mathbf{b}_{A,\Gamma^{ideal}(t)} = \mathbf{b} - A\mathbf{x}_{A,\mathbf{b},\Gamma^{ideal}(t)}, \quad (30)$$

where $\Gamma^{ideal}(t)$ is the active set at time t defined as

$$\Gamma^{ideal}(t) = \{j \in [\pm n] : A_j^\top \mathbf{v}^{ideal}(t) = 1\}. \quad (31)$$

Furthermore, we define $\mathbf{x}^{ideal}(t) := \mathbf{x}_{A,\mathbf{b},\Gamma^{ideal}(t)}$ be the local firing rate at time t .

As mentioned, we use ideal SNN to simulate a smoothed version of simple SNN with the spiking strength $\alpha \rightarrow 0$. The following theorem states that the local firing rate of the ideal SNN dynamics converges to an optimal solution of the ℓ_1 minimization problem, which we view as a partial evidence that simple SNN may solve the ℓ_1 minimization problem as well. We note that we consider local firing rate in the following theorem for simplicity. It is not hard to extend the conclusion to firing rate.

Theorem 5 (convergence of the ideal SNN dynamics). *Given $A \in \mathbb{R}^{m \times n}$ and $\mathbf{b} \in \mathbb{R}^m$ such that there exists a solution for $A\mathbf{x} = \mathbf{b}$. Let $\mathbf{x}(t)$ be the local firing rate of an ideal SNN. For any $t > 0$, $\mathbf{x}(t)$ is an $(\epsilon(t), \gamma(t))$ -approximate solution for the ℓ_1 minimization problem of (A, \mathbf{b}) where $\epsilon(t) = \frac{\text{OPT}^{\ell_1}}{t \cdot \|\mathbf{b}\|_2}$ and $\gamma(t) = \frac{\sqrt{n}}{t\sqrt{\lambda_{\min}}}$.*

We make the following discussion before proving the theorem.

The behavior of ideal SNN. Intuitively, we can understand the dynamics of ideal SNN as follows. We can view the dual vector $\mathbf{v}(t)$ as a ball initially located at the origin inside the feasible polytope at time $t = 0$, and there is a force that pushes the ball towards the \mathbf{b} direction with a constant speed. When the ball encounters some walls, it will move along the walls in the direction of conic projection of \mathbf{b} on the boundary of the feasible polytope, but at a slower speed depending on the angle between \mathbf{b} and its conic projection. At the end, the ball will reach and stay at the optimal corner \mathbf{v}^* .

Note that throughout the dynamics, the objective value $\mathbf{b}^\top \mathbf{v}(t)$ is monotonically increasing over time. This is in contrast to the “non-monotone” behavior of the simple SNN dynamics due to spikes. Also note that the speed may become arbitrarily slow if \mathbf{b} is very close to perpendicular to the walls. Thus, there is no explicit bound on the amount of time that $\mathbf{v}(t)$ reach the optimal corner \mathbf{v}^* . On the other hand, we note that when the speed becomes slow, it also means that the objective value is not too far from optimal.

Can we analyze simple SNN by coupling it with ideal SNN? Given Theorem 5, a natural approach to analyze simple SNN is to couple it with the ideal SNN dynamics. Unfortunately, we are not able to carry through this approach, again because of the complicated non-monotone behavior of spikes in simple SNN. Roughly, it is not clear how to bound the “distance” between the two dynamics.

Now, let us continue with the formal proof of Theorem 5.

6.3 Proof of Theorem 5

The proof of Theorem 5 consists of four steps: The first two steps build up some basic properties of the ideal SNN. Then, we prove the convergence of ℓ_2 norm in the third step. Finally, the convergence of ℓ_1 norm is proven in the last step. In the following, we are going to go through these four steps. Formal statements will be stated while some details will be put in the appendix.

Step 1: Connection between update rule and residual error Let’s start with some basic properties of the ideal SNN. Specifically, we build a connection between the update rule of $\mathbf{v}^{\text{ideal}}(t)$ and the residual error $\mathbf{b} - A\mathbf{x}^{\text{ideal}}$. Concretely, we have the following lemma.

Lemma 3. *For any $t \geq 0$, we have the following.*

1. $\mathbf{b}^\top A\mathbf{x}^{\text{ideal}}(t) = \|A\mathbf{x}^{\text{ideal}}(t)\|_2^2$,
2. $\|\mathbf{b} - A\mathbf{x}^{\text{ideal}}(t)\|_2^2 = \|\mathbf{b}\|_2^2 - \|A\mathbf{x}^{\text{ideal}}\|_2^2$, and
3. $\frac{d}{dt} \left(\mathbf{b}^\top \mathbf{v}^{\text{ideal}}(t) \right) = \|\mathbf{b}\|_2^2 - \|A\mathbf{x}^{\text{ideal}}(t)\|_2^2 = \|\mathbf{b} - A\mathbf{x}^{\text{ideal}}(t)\|_2^2$.

Proof of Lemma 3: The lemma is directly followed by the following property of conic projection. For any $A \in \mathbb{R}^{m \times n}$, $\mathbf{b} \in \mathbb{R}^m$, and $\Gamma \subseteq [\pm n]$ be a valid set, we have $\mathbf{b}^\top A \mathbf{x}_{A,\mathbf{b},\Gamma} = \|A \mathbf{x}_{A,\mathbf{b},\Gamma}\|_2^2$. In the following, we are going to first prove this property of conic projection and then use it to prove the lemma.

Let us rewrite the definition of conic projection as an optimization program.

$$\begin{aligned} & \underset{\mathbf{x} \in \mathbb{R}^n}{\text{minimize}} && \frac{1}{2} \|\mathbf{b} - A\mathbf{x}\|_2^2 \\ & \text{subject to} && \mathbf{x}_j \geq 0, \quad j \in \Gamma, \\ & && \mathbf{x}_i = 0, \quad i, -i \notin \Gamma. \end{aligned} \tag{32}$$

Let \mathbf{y} be the dual variable of (32) and \mathbf{y}^* be the optimal dual value, the Lagrangian of (32) is

$$\mathcal{L}(\mathbf{x}) = \frac{1}{2} \|\mathbf{b} - A\mathbf{x}\|_2^2 - \mathbf{y}^\top \mathbf{x}, \tag{33}$$

and its gradient is

$$\nabla_{\mathbf{x}} \mathcal{L}(\mathbf{x}) = A^\top A \mathbf{x} - A^\top \mathbf{b} - \mathbf{y}.$$

By the KKT condition, we know that the optimal primal solution $\mathbf{x}_{A,\mathbf{b},\Gamma}$ and the optimal dual solution \mathbf{y}^* make the gradient of the Lagrangian diminish.

$$\nabla_{\mathbf{x}} \mathcal{L}(\mathbf{x}_{A,\mathbf{b},\Gamma}) = A^\top A \mathbf{x}_{A,\mathbf{b},\Gamma} - A^\top \mathbf{b} - \mathbf{y}^* = 0, \tag{34}$$

and the complementary slackness

$$\mathbf{x}_{A,\mathbf{b},\Gamma}^\top \mathbf{y}^* = 0. \tag{35}$$

By (34) and (35), we have

$$(A \mathbf{x}_{A,\mathbf{b},\Gamma})^\top (\mathbf{b} - A \mathbf{x}_{A,\mathbf{b},\Gamma}) = 0. \tag{36}$$

As a result, $\mathbf{b}^\top A \mathbf{x}_{A,\mathbf{b},\Gamma} = \|A \mathbf{x}_{A,\mathbf{b},\Gamma}\|_2^2$.

With the above property of conic projection, the first two items of Lemma 3 are straightforward and the third item follows from Definition 5. ■

Intuitively, Lemma 3 can be interpreted as follows. The first two properties are results from the orthogonality of the conic projection. Recall that for ordinary projection, let $\bar{\mathbf{b}}$ be the projection of \mathbf{b} , we have $\bar{\mathbf{b}}$ being orthogonal to $\mathbf{b} - \bar{\mathbf{b}}$. It turns out this is also true for conic projection. With the orthogonality of conic projection, we can then prove the third statement in Lemma 3 about the update rule of ideal SNN. Intuitively, this connection tells us that the update rate of the objective function $\mathbf{b}^\top \mathbf{v}^{\text{ideal}}(t)$ is proportional to the ℓ_2 norm of the residual error. Namely, if the residual error is large, then the objective value $\mathbf{b}^\top \mathbf{v}^{\text{ideal}}(t)$ will grow fast.

However, the connection provided by Lemma 3 is a local property in the sense that the connection only concerns the behavior at an instant. That is, we cannot address the global property of the ideal SNN. For instance, we cannot infer how large the objective value is at t only given the information (*e.g.*, residual error) at time t . In the next step, we resolve this issue by showing the monotonicity of the residual error.

Step 2: Monotonicity of primal solution The following lemma shows the monotonicity of the residual error $\|\mathbf{b} - \mathbf{Ax}^{\text{ideal}}\|_2$.

Lemma 4. $\|\mathbf{b} - \mathbf{Ax}^{\text{ideal}}(t)\|_2$ is non-increasing and $\|\mathbf{Ax}^{\text{ideal}}(t)\|_2$ is non-decreasing in t .

Proof of Lemma 4: Consider two cases.

- (1) When there is a new index joins the active set. Clearly that $\|\mathbf{Ax}^{\text{ideal}}(t)\|_2$ won't decrease since the new cone contains the old one. By Lemma 4, we know that $\|\mathbf{b} - \mathbf{Ax}^{\text{ideal}}(t)\|_2$ is non-increasing.
- (2) When there is an index leaves the the active set. Without loss of generality, assume $j \in [\pm n]$ leaves the active set. In the following, we want to show that $\mathbf{x}_{|j|}^{\text{ideal}}(t) = 0$. As the direction of $\mathbf{v}^{\text{ideal}}(t)$ is $\mathbf{b} - \mathbf{Ax}^{\text{ideal}}(t)$, it means that $A_j^\top(\mathbf{b} - \mathbf{Ax}^{\text{ideal}}(t)) < 0$. Suppose $\mathbf{x}_{|j|}^{\text{ideal}}(t) \neq 0$ for contradiction. Since j was in the active set, it is the case that $\mathbf{x}_j^{\text{ideal}}(t) > 0$. Take $0 < \epsilon < \min\{\mathbf{x}_j^{\text{ideal}}(t)/2, -(\mathbf{b} - \mathbf{Ax}^{\text{ideal}}(t))^\top A_j / \|A_j\|_2\}$ and define $\mathbf{x}' = \mathbf{x}^{\text{ideal}}(t) - \epsilon \cdot A_j / \|A_j\|_2$. Note that \mathbf{x}' lies in the original active cone. Observe that

$$\begin{aligned} \|\mathbf{b} - \mathbf{Ax}'\|_2^2 &= \|\mathbf{b} - \mathbf{Ax}^{\text{ideal}}(t) + \epsilon \cdot A_j / \|A_j\|_2\|_2^2 \\ &= \|\mathbf{b} - \mathbf{Ax}^{\text{ideal}}(t)\|_2^2 + \|\epsilon \cdot A_j / \|A_j\|_2\|_2^2 + 2\epsilon \cdot (\mathbf{b} - \mathbf{Ax}^{\text{ideal}}(t))^\top A_j / \|A_j\|_2 \\ &\leq \|\mathbf{b} - \mathbf{Ax}^{\text{ideal}}(t)\|_2^2 + \epsilon^2 - 2\epsilon^2 \\ &< \|\mathbf{b} - \mathbf{Ax}^{\text{ideal}}(t)\|_2^2 \end{aligned}$$

which contradicts to the optimality of $\mathbf{x}^{\text{ideal}}(t)$ since \mathbf{x}' is also a feasible solution. We conclude that $\mathbf{x}_j^{\text{ideal}}(t) = 0$. As a result, $\mathbf{Ax}^{\text{ideal}}(t)$ remains the same and $\|\mathbf{Ax}^{\text{ideal}}(t)\|_2$ won't decrease. ■

Step 3: Convergence of ℓ_2 residual error Combine Lemma 3 and Lemma 4, we prove the convergence of residual error $\|\mathbf{b} - \mathbf{Ax}^{\text{ideal}}(t)\|_2$ by an *open-eyes-close-eyes argument*. The argument works as follows: Given some error ratio $\epsilon > 0$ we pick some $t > 0$ large enough. We open our eyes at time t . Then we assume the residual error is larger than $\epsilon \cdot \|\mathbf{b}\|_2$. By the monotonicity of residual error, we know that for any $1 \leq t' \leq t$, the residual error at time t' is also greater than $\epsilon \cdot \|\mathbf{b}\|_2$. As a result, by the connection of residual error and the update rule of ideal SNN in Lemma 4, we can have a lower bound for how large the objective value at time t is. By proper choice of t , we can simple make this lower bound exceed the optimal value \mathbf{OPT}^{ℓ_1} and result in a contradiction. Finally, we conclude that the residual error at time t is less than $\epsilon \cdot \|\mathbf{b}\|_2$ as we desire. See Lemma 5 and its proof for formal details.

Lemma 5. For any $\epsilon > 0$, when $t \geq \frac{\mathbf{OPT}^{\ell_1}}{\epsilon \cdot \|\mathbf{b}\|_2}$, $\|\mathbf{b} - \mathbf{Ax}^{\text{ideal}}(t)\|_2 \leq \epsilon \cdot \|\mathbf{b}\|_2$.

Proof of Lemma 5: Assume the statement is wrong, *i.e.*, $\|\mathbf{b} - \mathbf{Ax}^{\text{ideal}}(t)\|_2 > \epsilon \cdot \|\mathbf{b}\|_2$. Then by Lemma 4, for any $0 \leq s \leq t$,

$$\begin{aligned} \|\mathbf{b} - \mathbf{Ax}^{\text{ideal}}(s)\|_2^2 &= \|\mathbf{b}\|_2^2 - \|\mathbf{Ax}^{\text{ideal}}(s)\|_2^2 \\ &\geq \|\mathbf{b}\|_2^2 - \|\mathbf{Ax}^{\text{ideal}}(t)\|_2^2 \\ &= \|\mathbf{b} - \mathbf{Ax}^{\text{ideal}}(t)\|_2^2 > \epsilon^2 \cdot \|\mathbf{b}\|_2^2. \end{aligned}$$

Since $t \geq \frac{\mathbf{OPT}^{\ell_1}}{\epsilon \cdot \|\mathbf{b}\|_2}$, by Lemma 3,

$$\mathbf{b}^\top \mathbf{v}^{\text{ideal}}(t) = \int_0^t \mathbf{b}^\top d\mathbf{v}^{\text{ideal}}(s) > t \cdot \epsilon \cdot \|\mathbf{b}\|_2 \geq \mathbf{OPT}^{\ell_1}, \quad (37)$$

which is a contradiction to the optimality of \mathbf{OPT}^{ℓ_1} since $\mathbf{v}^{\text{ideal}}(t)$ is dual feasible of (25). As a result, we conclude that $\|\mathbf{b} - A\mathbf{x}^{\text{ideal}}(t)\|_2 \leq \epsilon \cdot \|\mathbf{b}\|_2$. ■

Step 4: Convergence to ℓ_1 minimization Finally, we are going to prove the convergence of the primal solution of ideal SNN to the ℓ_1 minimization problem. Note that the convergence here is in objective value instead of in the solution itself. Formally, we have the following lemma.

Lemma 6. *For any $t \geq 0$,*

$$\|\mathbf{x}^{\text{ideal}}(t)\|_1 - \mathbf{OPT}^{\ell_1} \leq \sqrt{\frac{n}{\lambda_{\min}}} \cdot \|\mathbf{b} - A\mathbf{x}^{\text{ideal}}(t)\|_2 \quad (38)$$

The proof of Lemma 6 consists of two steps. First, we show that the primal and the dual solution pair of ideal SNN at time t is the optimal solution pair of a *perturbed ℓ_1 minimization problem* defined as shifting the \mathbf{b} in the constraint $A\mathbf{x} = \mathbf{b}$ to $A\mathbf{x}^{\text{ideal}}(t)$. See (39) for the definition of the perturbed program. Next, by the standard perturbation theorem from optimization, we can upper bound $\|\mathbf{x}^{\text{ideal}}(t)\|_1$ with the distance between the original program and the perturbed program. Specifically, the difference induced by the perturbation is related to the ℓ_2 norm of the difference between \mathbf{b} and $A\mathbf{x}^{\text{ideal}}(t)$, which is exactly the residual error. As a result, we know that the difference between the optimal value of the original ℓ_1 minimization program and that of the perturbed program will converge to 0. Namely, we yield a convergence of $\|\mathbf{x}^{\text{ideal}}(t)\|_1$ to \mathbf{OPT}^{ℓ_1} .

Proof of Lemma 6: For any $t \geq 0$, define the following perturbed program of (24) and its dual.

$$\begin{array}{ll} \underset{\mathbf{x}}{\text{minimize}} & \|\mathbf{x}\|_1 \\ \text{subject to} & A\mathbf{x} - A\mathbf{x}^{\text{ideal}}(t) = 0 \end{array} \quad (39) \quad \begin{array}{ll} \underset{\mathbf{v} \in \mathbb{R}^m}{\text{maximize}} & (A\mathbf{x}^{\text{ideal}}(t))^\top \mathbf{v} \\ \text{subject to} & \|A^\top \mathbf{v}\|_\infty \leq 1. \end{array} \quad (40)$$

Note that $\mathbf{x}^{\text{ideal}}(t)$ is treated as a given constant to the optimization program. It turns out that the ideal algorithm optimizes this primal-dual perturbed program at time t with the following parameters.

Lemma 7. *For any $t \geq 0$, $(\mathbf{x}^*, \mathbf{v}^*) = (\mathbf{x}^{\text{ideal}}(t), \mathbf{v}^{\text{ideal}}(t))$ is the optimal solutions of (39).*

Proof of Lemma 7: We simply check the KKT condition. Since the program can be rewritten as a linear program, it satisfies the regularity condition of the KKT condition.

First, the primal and the dual feasibility can be verified by the dynamics of ideal algorithm. That is, $A\mathbf{x}^* - A\mathbf{x}^{\text{ideal}}(t) = 0$ and $\|A^\top \mathbf{v}^*\|_\infty \leq 1$. Next, consider the Lagrangian of (39) as follows.

$$\begin{aligned} \mathcal{L}(\mathbf{x}, \mathbf{v}) &= \|\mathbf{x}\|_1 - \mathbf{v}^\top (A\mathbf{x} - A\mathbf{x}^{\text{ideal}}(t)), \\ \nabla_{\mathbf{x}} \mathcal{L}(\mathbf{x}, \mathbf{v}) &= \nabla \|\mathbf{x}\|_1 - A^\top \mathbf{v}. \end{aligned}$$

Now, let's verify that the gradient of the Lagrangian over \mathbf{x} is vanishing at $(\mathbf{x}^*, \mathbf{v}^*) = (\mathbf{x}^{\text{ideal}}(t), \mathbf{v}^{\text{ideal}}(t))$. That is, $0 \in \nabla_{\mathbf{x}} \mathcal{L}(\mathbf{x}^*, \mathbf{v}^*) = \nabla \|\mathbf{x}\|_1 - A^\top \mathbf{v}^*$. Consider two cases as follows. For any $i \in [n]$,

- (1) When $i, -i \notin \Gamma^{\text{ideal}}(t)$. We have $\left(\mathbf{x}^{\text{ideal}}(t)\right)_i = 0$, *i.e.*, the sub-gradient of the i th coordinate of $\|\mathbf{x}^{\text{ideal}}(t)\|_1$ lies in $[-1, 1]$. As $A_i^\top \mathbf{v}^{\text{ideal}}(t) \in [-1, 1]$, we have $A_i^\top \mathbf{v}^{\text{ideal}}(t) \in \partial_{\mathbf{x}_i} \|\mathbf{x}^{\text{ideal}}(t)\|_1$.
- (2) When $i \in \Gamma^{\text{ideal}}(t)$ (or $-i \in \Gamma^{\text{ideal}}(t)$). We have $A_i^\top \mathbf{v}^{\text{ideal}}(t) = 1$ (or $A_i^\top \mathbf{v}^{\text{ideal}}(t) = -1$). As $\text{sgn}\left(\mathbf{x}^{\text{ideal}}(t)\right)_i = 1$ (or $\text{sgn}\left(\mathbf{x}^{\text{ideal}}(t)\right)_i = -1$), we have $A_i^\top \mathbf{v}^{\text{ideal}}(t) = \text{sgn}\left(\mathbf{x}^{\text{ideal}}(t)\right)_i = \partial_{\mathbf{x}_i} \|\mathbf{x}^{\text{ideal}}(t)\|_1$.

Finally, the complementary slackness is satisfied because $A\mathbf{x}^* - A\mathbf{x}^{\text{ideal}}(t) = 0$. As a result, we conclude that $(\mathbf{x}^*, \mathbf{v}^*)$ is the optimal solution of (39). \blacksquare

Next, we are going to use the perturbation lemma in the Chapter 5.6 of [BV04] stated below.

Lemma 8 (perturbation lemma). *Given the following two optimization programs.*

$$\begin{aligned} \underset{\mathbf{x}}{\text{minimize}} \quad & f(\mathbf{x}) & \underset{\mathbf{x}}{\text{minimize}} \quad & f(\mathbf{x}) \\ \text{subject to} \quad & h(\mathbf{x}) = \mathbf{0}. & \text{subject to} \quad & h(\mathbf{x}) = \mathbf{y}. \end{aligned} \quad (41) \qquad (42)$$

Let $\mathbf{OPT}^{\text{original}}$ be the optimal value of the original program (41) and $\mathbf{OPT}^{\text{perturbed}}$ be the optimal value of the perturbed program (42). Let \mathbf{v}^* be the optimal dual value of the perturbed program (42). We have

$$\mathbf{OPT}^{\text{original}} \geq \mathbf{OPT}^{\text{perturbed}} + \mathbf{y}^\top \mathbf{v}^*. \quad (43)$$

Now, think of (24) as the original program and (39) as the perturbed program. Namely, $f(\mathbf{x}) = \|\mathbf{x}\|_1$, $h(\mathbf{x}) = A\mathbf{x} - \mathbf{b}$, and $\mathbf{y} = A\mathbf{x}^{\text{ideal}}(t) - \mathbf{b}$. By the perturbation lemma, we have

$$\mathbf{OPT}^{\ell_1} \geq \|\mathbf{x}^{\text{ideal}}(t)\|_1 + \left(A\mathbf{x}^{\text{ideal}}(t) - \mathbf{b}\right)^\top \mathbf{v}^{\text{ideal}}(t).$$

As a result, the following upper bound holds.

$$\|\mathbf{x}^{\text{ideal}}(t)\|_1 \leq \mathbf{OPT}^{\ell_1} + \|\mathbf{v}^{\text{ideal}}(t)\|_2 \cdot \|\mathbf{b} - A\mathbf{x}^{\text{ideal}}(t)\|_2. \quad (44)$$

Finally, as $\mathbf{v}^{\text{ideal}}(t)$ lies in the feasible region $\{\mathbf{v} : A^\top \mathbf{v}\|_\infty \leq 1\}$ and the range space of A , we can upper bound the $\|\mathbf{v}^{\text{ideal}}(t)\|_2$ term in (44) as follows.

Lemma 9. *For any \mathbf{v} in the range space of A and $\|A^\top \mathbf{v}\|_\infty \leq 1$, $\|\mathbf{v}\|_2 \leq \sqrt{\frac{n}{\lambda_{\min}}}$.*

Proof of Lemma 9: As \mathbf{v} lies in the range space of A , we have $\|A^\top \mathbf{v}\|_2 \geq \sqrt{\lambda_{\min}} \|\mathbf{v}\|_2$. Also, because $\|A^\top \mathbf{v}\|_\infty \leq 1$, we have $\|A^\top \mathbf{v}\|_2 \leq \sqrt{n}$. As a result,

$$\|\mathbf{v}\|_2 \leq \frac{\|A^\top \mathbf{v}\|_2}{\sqrt{\lambda_{\min}}} \leq \sqrt{\frac{n}{\lambda_{\min}}}.$$

By (44) and Lemma 9, Lemma 6 holds. \blacksquare

Proof of Theorem 5: Theorem 5 simply follows from Lemma 5 and Lemma 6. \blacksquare

6.4 SNN simulations

In this section, we start with running SNN algorithm on commonly used matrices to argue the good empirical performance of SNN on ℓ_1 minimization problem. Next, we present two bad matrices to illustrate the difficulty of proving the convergence to ℓ_1 minimization problem. Note that as this is a theoretical paper, the simulations are not optimized and our purpose is to inspire future study and highlight the difficulties.

6.4.1 Commonly used inputs

In many situations of encountering ℓ_1 minimization problem, the matrix A has some good properties. For instance, in compressed sensing [Don06, C+06], people use matrices with *restricted isometry property (RIP)* or with low mutual incoherence. Here, we focus on these well-structured matrices and run SNN algorithm on them. We discover that simple SNN behaves well in the case where A is a normalized random matrix and the solution is very sparse.

Let n be a variable scaling from 128 to 13762 and $m = \lfloor n/4 \rfloor$. Define A to be a $n \times m$ matrix normalized Gaussian matrix in the sense that every entry of A is sampled from standard Gaussian distribution and the eigenvalue of A is scaled to either 1 or 0. Pick the optimal solution \mathbf{x}^* to be a random sparse vector with constant (here we chose 20) number of nonzero entries (here we set all of them to either 1 or -1). See Figure 7 for the simulation result. Our testing environment was a Mac running OS X EI Capitan 64 bit version with Intel Core i5 CPU 2.7GHz and 8GB RAM.

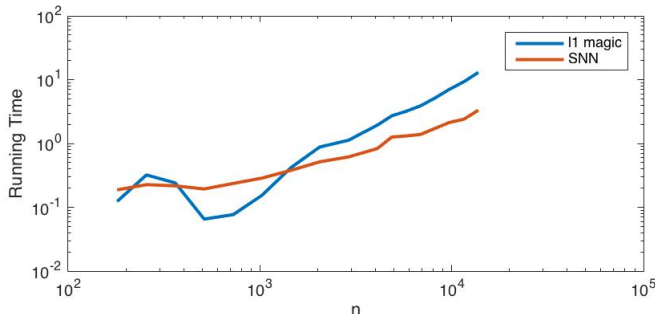


Figure 7: We compare the SNN algorithm with the ℓ_1 -magic [CR05a] over normalized Gaussian matrix. In the simulation, we fixed the tolerating error (10^{-3}) and run the two algorithms.

In the simulation, we only consider the asymptotic behavior with respect to the growing of n . One can see that when n becomes large, the slope of the two lines are almost the same. We point out that the experiment in Figure 7 is an easy case in the sense that the SNN algorithm finds the correct active set in the very beginning and starts to converge. For complicated case, *e.g.*, the examples introduced later, SNN algorithm might perform badly in the beginning. From this example, we want to assert that SNN algorithm performs well on the easy case and could probably be useful for practical usage.

Remark 2. As we know from the natural of firing rate, the error dependency is $\Omega(1/\epsilon)$ while the error dependency of ℓ_1 -magic is $O(\log 1/\epsilon)$. As a result, it is difficult for SNN to compare with ℓ_1 -magic in small error region such as 10^{-8} . Thus, here we consider large error region where the relative error is 10^{-3} . In this region, SNN outperforms ℓ_1 magic when n is greater than 2000.

6.4.2 Bad inputs

Here we are going to present two examples where the SNN algorithm does not perform well. As we mentioned before, the difficulty of proving simple SNN solving the ℓ_1 minimization problem lies in the lack of monotone behavior. In the following examples, we are going to focus on the non-monotone behavior of simple SNN to demonstrate the difficulty. Both examples make simple SNN have a bad behavior in the beginning of the executions. Specifically, error might increase in the beginning and it takes time to correct the bad start. Moreover, it is also unknown how to estimate how long the bad start will last.

Wrong direction in the beginning Let $n \geq 3$, $m = n$, and $0 < \epsilon < 0.1$. Define $A \in \mathbb{R}^{n \times n}$, $\mathbf{x}^* \in \mathbb{R}^n$, and $\mathbf{b} \in \mathbb{R}^n$ as follows.

$$A = \begin{pmatrix} 1 & \sqrt{1-\epsilon^2} & \sqrt{1-\epsilon^2} & \cdots & \sqrt{1-\epsilon^2} \\ 0 & \epsilon & 0 & \cdots & 0 \\ 0 & 0 & \epsilon & \cdots & 0 \\ \vdots & \vdots & \vdots & \ddots & \vdots \\ 0 & 0 & 0 & \cdots & \epsilon \end{pmatrix}, \mathbf{x}^* = \begin{pmatrix} -1 \\ 1 \\ 1 \\ \vdots \\ 1 \end{pmatrix}, \mathbf{b} = A\mathbf{x}^* = \begin{pmatrix} (n-1) \cdot \sqrt{1-\epsilon^2} - 1 \\ \epsilon \\ \epsilon \\ \vdots \\ \epsilon \end{pmatrix}$$

In this example, the optimal solution is \mathbf{x}^* so that the first neuron should fire negative spikes and the other neurons should fire positive spikes. However, in the Figure 8, the first neuron fires positive spikes in the beginning. That is, the output by the SNN algorithm in the beginning has a wrong sign in the first column.

One reason to explain this phenomenon is that all column vectors of A are highly correlated with each other. That is, the polytope \mathcal{P}_A is extremely *astute*. As a result, the inner product of \mathbf{b} with the first column vector of A is actually positive, which is the opposite of the sign of the first entry of \mathbf{x}^* . Namely, the external charging of the dual SNN, *i.e.*, \mathbf{b} , is actually making the first neuron more likely to fire a positive spike.

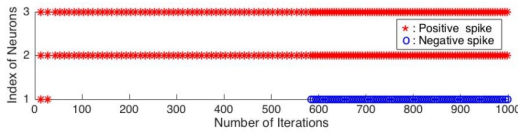


Figure 8: In the first example, the first neuron fires positive spikes in the beginning while the optimal solution is negative at the first coordinate.

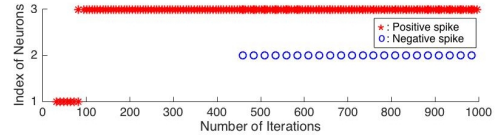


Figure 9: In the second example, the first neuron fires some positive spikes in the beginning while the optimal solution is zero at the first coordinate.

Wrong neuron in the beginning Let $n = 3$ and $m = 2$. Define $A \in \mathbb{R}^{m \times n}$, $\mathbf{b} \in \mathbb{R}^m$ as follows.

$$A = \begin{pmatrix} 0.7 & 0.5 & 0.6 \\ -0.3 & -0.5 & -0.1 \end{pmatrix}, \mathbf{b} = \begin{pmatrix} 1 \\ 0 \end{pmatrix}.$$

The optimal solution of the ℓ_1 minimization problem with A and \mathbf{b} defined above is $(0, -0.4, 2)^\top$. That is, only the second and the third neurons are active. However, the first neuron will be the

one which fires the first spike. See Figure 9 for the razor plot of the simulation. A geometric angle to view this example is as follows: For any $\Gamma \subseteq [\pm n]$, define the primal cone of Γ with respect to A as $C_{A,\Gamma} := \{\mathbf{v} = \sum_{i \in \Gamma} A_i a_i, \forall a_i \geq 0\}$. Note that \mathbf{b} must lie in the primal cone of Γ^* , which is the active set of the optimal dual solution \mathbf{v}^* . Ideally, as the dual SNN moves along \mathbf{b} , we hope that it only hits the walls from Γ^* . However, in this example, there is another wall, W_1 , that cut through the primal cone of Γ^* . As a result, the dual SNN hit W_1 before getting close to \mathbf{v}^* . See Figure 10 and Figure 11 for illustration.

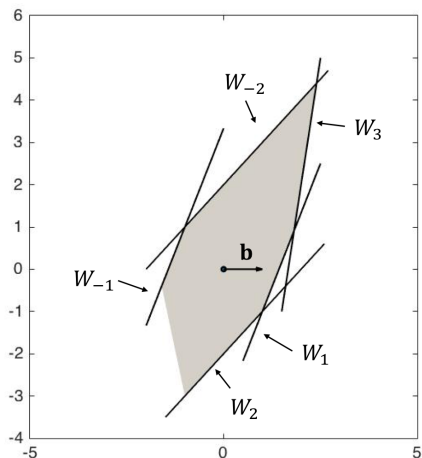


Figure 10: This is the dual space of the second example where the dual SNN will first hit a non-optimal wall.

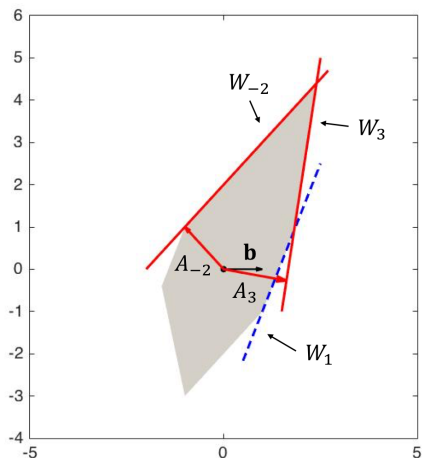


Figure 11: There is a non-optimal wall (blue dotted line) cutting through the optimal primal cone

To sum up, we point out that the above two bad examples can serve as a good sanity check when coming up with a proof for the convergence of simple SNN to the ℓ_1 minimization problem. Also, by examining these two examples deeply, we hope it can help to build intuition for the dynamics of simple SNN. We encourage people who are interested in continuing this line of work to study these examples thoroughly.

Acknowledgements. The authors would like to thank Tsung-Han Lin, Zhenming Liu, Luca Trevisan, Richard Peng, Yin-Hsun Huang, and Tao Xiao for useful discussions related to this paper.

References

- [Adr26] Edgar D Adrian. The impulses produced by sensory nerve endings. *The Journal of physiology*, 61(1):49–72, 1926.
- [BDM13] David G Barrett, Sophie Denève, and Christian K Machens. Firing rate predictions in optimal balanced networks. In *Advances in Neural Information Processing Systems*, pages 1538–1546, 2013.

- [BIP15] Jonathan Binas, Giacomo Indiveri, and Michael Pfeiffer. Spiking analog vlsi neuron assemblies as constraint satisfaction problem solvers. *arXiv preprint arXiv:1511.00540*, 2015.
- [BMV12] Vincenzo Bonifaci, Kurt Mehlhorn, and Girish Varma. Physarum can compute shortest paths. *Journal of Theoretical Biology*, 309:121–133, 2012.
- [BPLG16] Anmol Biswas, Sidharth Prasad, Sandip Lashkare, and Udayan Ganguly. A simple and efficient snn and its performance & robustness evaluation method to enable hardware implementation. *arXiv preprint arXiv:1612.02233*, 2016.
- [BT09] Amir Beck and Marc Teboulle. A fast iterative shrinkage-thresholding algorithm for linear inverse problems. *SIAM journal on imaging sciences*, 2(1):183–202, 2009.
- [BV04] Stephen Boyd and Lieven Vandenberghe. *Convex optimization*. Cambridge university press, 2004.
- [C⁺06] Emmanuel J Candès et al. Compressive sampling. In *Proceedings of the international congress of mathematicians*, volume 3, pages 1433–1452. Madrid, Spain, 2006.
- [CDS01] Scott Shaobing Chen, David L Donoho, and Michael A Saunders. Atomic decomposition by basis pursuit. *SIAM review*, 43(1):129–159, 2001.
- [Cha09] Bernard Chazelle. Natural algorithms. In *Proceedings of the twentieth Annual ACM-SIAM Symposium on Discrete Algorithms*, pages 422–431. Society for Industrial and Applied Mathematics, 2009.
- [Cha12] Bernard Chazelle. Natural algorithms and influence systems. *Communications of the ACM*, 55(12):101–110, 2012.
- [CR05a] Emmanuel C and Justin Romberg. l1-magic: Recovery of sparse signals via convex programming, 2005.
- [CR05b] Emmanuel Candes and Justin Romberg. l1-magic: Recovery of sparse signals via convex programming. *URL: www.acm.caltech.edu/l1magic/downloads/l1magic.pdf*, 4:14, 2005.
- [Don06] David L Donoho. Compressed sensing. *IEEE Transactions on information theory*, 52(4):1289–1306, 2006.
- [HH52] Alan L Hodgkin and Andrew F Huxley. A quantitative description of membrane current and its application to conduction and excitation in nerve. *The Journal of physiology*, 117(4):500, 1952.
- [I⁺03] Eugene M Izhikevich et al. Simple model of spiking neurons. *IEEE Transactions on neural networks*, 14(6):1569–1572, 2003.
- [JHM16] Zeno Jonke, Stefan Habenschuss, and Wolfgang Maass. Solving constraint satisfaction problems with networks of spiking neurons. *Frontiers in neuroscience*, 10, 2016.

- [Lap07] Louis Lapicque. Recherches quantitatives sur l'excitation électrique des nerfs traitée comme une polarisation. *J. Physiol. Pathol. Gen.*, 9(1):620–635, 1907.
- [LP16] Adi Livnat and Christos Papadimitriou. Sex as an algorithm: the theory of evolution under the lens of computation. *Communications of the ACM*, 59(11):84–93, 2016.
- [LPR⁺14] Adi Livnat, Christos Papadimitriou, Aviad Rubinfeld, Gregory Valiant, and Andrew Wan. Satisfiability and evolution. In *Foundations of Computer Science (FOCS), 2014 IEEE 55th Annual Symposium on*, pages 524–530. IEEE, 2014.
- [Maa14] Wolfgang Maass. Noise as a resource for computation and learning in networks of spiking neurons. *Proceedings of the IEEE*, 102(5):860–880, 2014.
- [Maa15] Wolfgang Maass. To spike or not to spike: That is the question. *Proceedings of the IEEE*, 103(12):2219–2224, 2015.
- [MMI15] Hesham Mostafa, Lorenz K Müller, and Giacomo Indiveri. An event-based architecture for solving constraint satisfaction problems. *Nature communications*, 6, 2015.
- [NYT00] Toshiyuki Nakagaki, Hiroyasu Yamada, and Ágota Tóth. Intelligence: Maze-solving by an amoeboid organism. *Nature*, 407(6803):470–470, 2000.
- [PMB12] Héline Paugam-Moisy and Sander Bohte. Computing with spiking neuron networks. In *Handbook of natural computing*, pages 335–376. Springer, 2012.
- [RJBO08] Christopher J Rozell, Don H Johnson, Richard G Baraniuk, and Bruno A Olshausen. Sparse coding via thresholding and local competition in neural circuits. *Neural computation*, 20(10):2526–2563, 2008.
- [SRH13] Samuel Shapero, Christopher Rozell, and Paul Hasler. Configurable hardware integrate and fire neurons for sparse approximation. *Neural Networks*, 45:134–143, 2013.
- [Ste65] Richard B Stein. A theoretical analysis of neuronal variability. *Biophysical Journal*, 5(2):173, 1965.
- [SZHR14] Samuel Shapero, Mengchen Zhu, Jennifer Hasler, and Christopher Rozell. Optimal sparse approximation with integrate and fire neurons. *International journal of neural systems*, 24(05):1440001, 2014.
- [TKN07] Atsushi Tero, Ryo Kobayashi, and Toshiyuki Nakagaki. A mathematical model for adaptive transport network in path finding by true slime mold. *Journal of theoretical biology*, 244(4):553–564, 2007.
- [TLD17] Ping Tak Peter Tang, Tsung-Han Lin, and Mike Davies. Sparse coding by spiking neural networks: Convergence theory and computational results. *arXiv preprint arXiv:1705.05475*, 2017.
- [YSGM10] Allen Y Yang, S Shankar Sastry, Arvind Ganesh, and Yi Ma. Fast l1-minimization algorithms and an application in robust face recognition: A review. In *2010 IEEE International Conference on Image Processing*, pages 1849–1852. IEEE, 2010.

7 Lemmas for Theorem 3

7.1 Proof of Lemma 1

In the following, we are going to prove two properties of matrix norm. First, for any $\mathbf{x} \in \mathbb{R}^n$, $\|\mathbf{x}\|_{A^\top A} = \|\mathbf{Ax}\|_2 = \|A^\top \mathbf{Ax}\|_{(A^\top A)^\dagger}$. Second, $\|A^\top \mathbf{b}\|_{(A^\top A)^\dagger} = \|\mathbf{b}_A\|_2$.

1. It is easy to see that by definition, $\|\mathbf{x}\|_{A^\top A} = \|\mathbf{Ax}\|_2$. As to the second equality, first recall that if a vector $\mathbf{v} \in \mathbb{R}^n$ lies in the range space of $A^\top A$, then

$$(A^\top A)^\dagger (A^\top A) \mathbf{v} = \mathbf{v}. \quad (45)$$

Let \mathbf{x}_A be the projection of \mathbf{x} such that $A^\top \mathbf{Ax} = A^\top \mathbf{Ax}_A$ and \mathbf{x}_A lies in the range space of $A^\top A$. By (45), we have

$$\begin{aligned} \|A^\top \mathbf{Ax}\|_{(A^\top A)^\dagger}^2 &= (A^\top \mathbf{Ax})^\top (A^\top A)^\dagger (A^\top \mathbf{Ax}) \\ &= (A^\top \mathbf{Ax}_A)^\top (A^\top A)^\dagger (A^\top \mathbf{Ax}_A) \\ &= (A^\top \mathbf{Ax}_A)^\top \mathbf{x}_A \\ &= \|\mathbf{Ax}_A\|_2^2 = \|\mathbf{Ax}\|_2^2. \end{aligned}$$

2. Let $\mathbf{x} \in \mathbb{R}^n$ be a solution of $\mathbf{Ax} = \mathbf{b}_A$ ¹⁵ and define \mathbf{x}_A as we did in the first item. By (45), we have

$$\begin{aligned} \|A^\top \mathbf{b}\|_{(A^\top A)^\dagger}^2 &= (A^\top \mathbf{b})^\top (A^\top A)^\dagger (A^\top \mathbf{b}) \\ &= (A^\top \mathbf{Ax}_A)^\top (A^\top A)^\dagger (A^\top \mathbf{Ax}_A) \\ &= \|\mathbf{Ax}_A\|_2^2 = \|\mathbf{b}_A\|_2^2. \end{aligned}$$

7.2 Proof of Lemma 2

At timestep t , denote the set of neurons that are exceeding threshold as $\Gamma(t) := \{i \in [n] \mid |\mathbf{u}_i(t)| > \lambda\}$. We have the following observation.

Lemma 10. *For any $t \in \mathbb{N}$, $\mathbf{u}(t)^\top \mathbf{s}(t) \geq \eta \cdot |\Gamma(t)|$ ¹⁶.*

Proof. Observe that

$$\mathbf{u}(t)^\top \mathbf{s}(t) = \sum_{i \in [n]} \mathbf{u}_i(t) \cdot \mathbf{s}(t) \quad (46)$$

$$= \sum_{i \in \Gamma(t)} \mathbf{u}_i(t) \cdot \text{sign}(\mathbf{u}_i(t)) = \sum_{i \in \Gamma(t)} |\mathbf{u}_i(t)| \quad (47)$$

$$\geq \sum_{i \in \Gamma(t)} \eta = \eta \cdot |\Gamma(t)|. \quad (48)$$

■

¹⁵Note that this is possible since \mathbf{b}_A lies in the range space of $A^\top A$.

¹⁶It is not difficult to see that when $|\Gamma(t)| \neq 0$, it is actually $\mathbf{u}(t)^\top \mathbf{s}(t) > \eta \cdot |\Gamma(t)|$

Lemma 11. For any $t \in \mathbb{N}$, $\mathbf{u}(t)^\top (A^\top A)^\dagger A^\top \mathbf{A} \mathbf{s}(t) = \mathbf{u}(t)^\top \mathbf{s}(t)$.

Proof. First, note that $(A^\top A)^\dagger A^\top A$ is the orthogonal projection matrix of the range space of $A^\top A$. Next, by the dynamics of SNN and $\mathbf{u}(1) = \mathbf{0}$, we know that $\mathbf{u}(t)$ is in the range space of $A^\top A$. Let $\mathbf{z} \in \mathbb{R}^n$ be the unique vector in the range space of $A^\top A$ such that $\mathbf{u}(t) = A^\top A \mathbf{z}(t)$. Let $\mathbf{s}_A(t)$ be the projection of $\mathbf{s}(t)$ in the range space of $A^\top A$. Note that $A^\top \mathbf{A} \mathbf{s}(t) = A^\top \mathbf{A} \mathbf{s}_A(t)$. By Lemma 1, we have

$$\begin{aligned} \mathbf{u}(t)^\top (A^\top A)^\dagger A^\top \mathbf{A} \mathbf{s}(t) &= \mathbf{z}^\top A^\top A (A^\top A)^\dagger A^\top \mathbf{A} \mathbf{s}_A(t) \\ &= \mathbf{z}^\top A^\top \mathbf{A} \mathbf{s}_A(t) \\ &= \mathbf{z}^\top A^\top \mathbf{A} \mathbf{s}(t) = \mathbf{u}(t)^\top \mathbf{s}(t). \end{aligned}$$

■

We now prove Lemma 2 using Lemma 10 and Lemma 11.

Proof of Lemma 2: The proof is based on an induction over the number of iterations $t \in \mathbb{N}$. Let $B = 2\sqrt{\kappa \cdot \eta \cdot \bar{n}}$, our goal is to show that $\|\mathbf{u}(t)\|_{(A^\top A)^\dagger} \leq B$ for any t when $\Delta t \leq \frac{\sqrt{\lambda_{\min}}}{24 \cdot \sqrt{\bar{n}} \cdot \|\mathbf{b}_A\|_2}$. Clearly that $\|\mathbf{u}(1)\|_{(A^\top A)^\dagger} = 0 \leq B$, assume $\|\mathbf{u}(t)\|_{(A^\top A)^\dagger} \leq B$, consider

$$\|\mathbf{u}(t+1)\|_{(A^\top A)^\dagger}^2 = \|\mathbf{u}(t) - A^\top \mathbf{A} \mathbf{s}(t) + A^\top \mathbf{b} \cdot \Delta t\|_{(A^\top A)^\dagger}^2 \quad (49)$$

$$\begin{aligned} &= \|\mathbf{u}(t)\|_{(A^\top A)^\dagger}^2 + \|A^\top \mathbf{A} \mathbf{s}(t) - A^\top \mathbf{b} \cdot \Delta t\|_{(A^\top A)^\dagger}^2 \\ &\quad - 2\mathbf{u}(t)^\top (A^\top A)^\dagger (A^\top \mathbf{A} \mathbf{s}(t) - A^\top \mathbf{b} \cdot \Delta t). \end{aligned} \quad (50)$$

Expand the $\|A^\top \mathbf{A} \mathbf{s}(t) - A^\top \mathbf{b} \cdot \Delta t\|_{(A^\top A)^\dagger}^2$ term, by Lemma 1, we have

$$\|A^\top \mathbf{A} \mathbf{s}(t) - A^\top \mathbf{b} \cdot \Delta t\|_{(A^\top A)^\dagger}^2 = \|\mathbf{A} \mathbf{s}(t) - \mathbf{b}_A \cdot \Delta t\|_2^2 \quad (51)$$

$$\leq \|\mathbf{A} \mathbf{s}(t)\|_2^2 + \|\mathbf{b}_A \cdot \Delta t\|_2^2 - 2\mathbf{s}(t)^\top A^\top \mathbf{b} \cdot \Delta t \quad (52)$$

$$\leq \lambda_{\max} |\Gamma(t)| + \|\mathbf{b}_A\|_2^2 \cdot \Delta t^2 + 2\sqrt{\lambda_{\max} \cdot |\Gamma(t)|} \|\mathbf{b}_A\|_2 \cdot \Delta t. \quad (53)$$

The last inequality is from Cauchy-Schwartz inequality and the fact that $\|\mathbf{s}(t)\|_2^2 = |\Gamma(t)|$. Next, by Lemma 10, Lemma 11, Cauchy-Schwartz inequality, and the induction hypothesis, we have

$$-2\mathbf{u}(t)^\top (A^\top A)^\dagger (A^\top \mathbf{A} \mathbf{s}(t) - A^\top \mathbf{b} \cdot \Delta t) = -2\mathbf{u}(t)^\top \mathbf{s}(t) + 2\|\mathbf{u}(t)\|_{(A^\top A)^\dagger} \cdot \|A^\top \mathbf{b}_A\|_{(A^\top A)^\dagger} \cdot \Delta t. \quad (54)$$

$$= -2\mathbf{u}(t)^\top \mathbf{s}(t) + 2\|\mathbf{u}(t)\|_{(A^\top A)^\dagger} \cdot \|\mathbf{b}_A\|_2 \cdot \Delta t. \quad (55)$$

$$\leq -2\eta |\Gamma(t)| + 2B \|\mathbf{b}_A\|_2 \cdot \Delta t. \quad (56)$$

The second equality is by Lemma 11. Combine (50), (53), (56), and induction hypothesis, we have

$$\begin{aligned} \|\mathbf{u}(t+1)\|_{(A^\top A)^\dagger}^2 &= \|\mathbf{u}(t)\|_{(A^\top A)^\dagger}^2 + (\lambda_{\max} - 2\eta) \cdot |\Gamma(t)| \\ &\quad + (2\sqrt{\lambda_{\max} |\Gamma(t)|} \cdot \|\mathbf{b}_A\|_2 + 2B \cdot \|\mathbf{b}_A\|_2) \cdot \Delta t + \|\mathbf{b}_A\|_2^2 \cdot \Delta t^2. \end{aligned}$$

By the choice of $\eta, \Delta t$, and B , we have

$$\|\mathbf{u}(t+1)\|_{(A^\top A)^\dagger}^2 \leq \|\mathbf{u}(t)\|_{(A^\top A)^\dagger}^2 - \lambda_{\max} \cdot |\Gamma(t)| + \frac{\sqrt{\lambda_{\max} \lambda_{\min} |\Gamma(t)|}}{6\sqrt{\bar{n}}} + \frac{\lambda_{\max}}{6} + \frac{\lambda_{\min}}{144\bar{n}} \quad (57)$$

$$\leq \|\mathbf{u}(t)\|_{(A^\top A)^\dagger}^2 - \lambda_{\max} |\Gamma(t)| + \frac{\lambda_{\max} |\Gamma(t)|}{2} + \frac{\lambda_{\max}}{2}. \quad (58)$$

Now, there are two cases to consider: $\Gamma(t)$ is empty or not. From (58) we can see that if $\Gamma(t)$ is nonempty, then by the induction hypothesis, $\|\mathbf{u}(t+1)\|_{(A^\top A)^\dagger} \leq \|\mathbf{u}(t)\|_{(A^\top A)^\dagger} \leq B$. If $\Gamma(t)$ is empty, then for any $i \in [n]$, $|\mathbf{u}_i(t)| \leq \eta$. Thus, we have

$$\|\mathbf{u}(t+1)\|_{(A^\top A)^\dagger} \leq \|\mathbf{u}(t)\|_{(A^\top A)^\dagger} + \frac{\lambda_{\max}}{2}. \quad (59)$$

Since $|\Gamma(t)| = 0$, we know that $\|\mathbf{u}(t)\|_\infty \leq \eta$ and thus

$$\|\mathbf{u}(t)\|_{(A^\top A)^\dagger}^2 \leq \frac{\|\mathbf{u}(t)\|_2^2 \leq n \cdot \max_{i \in [n]} |\mathbf{u}_i(t)|^2}{\lambda_{\min}} \leq \frac{\eta^2 n}{\lambda_{\min}}.$$

As a result, for the $|\Gamma(t)| = 0$ case, we have

$$\begin{aligned} \|\mathbf{u}(t+1)\|_{(A^\top A)^\dagger} &\leq \|\mathbf{u}(t)\|_{(A^\top A)^\dagger} + \frac{\lambda_{\max}}{2} \\ &\leq \frac{\eta\sqrt{n}}{\sqrt{\lambda_{\min}}} + \frac{B}{2} \\ &\leq \sqrt{\kappa\eta n} + \frac{B}{2} \leq B. \end{aligned}$$

We conclude that the induction holds and thus Lemma 2 is proved. ■

8 Proofs for stochastic SNN

Recall that $f(\mathbf{x}) := \frac{1}{2} \|\mathbf{b}_A - A\mathbf{x}\|_2^2$ is the objective function of the least square problem and its gradient is $\nabla f(\mathbf{x}) = A^\top A\mathbf{x} - A^\top \mathbf{b}$. The minimum ℓ_2 solution is denoted as $\mathbf{x}^{\ell_2} := \arg \min_{\mathbf{x}: A\mathbf{x}=\mathbf{b}_A} \|\mathbf{x}\|_2$. The parameters are chosen to be $\eta = \Omega(\|\mathbf{x}^{\ell_2}\|_2)$, $\alpha = O(\frac{\eta}{\kappa\lambda_{\max}n \ln \frac{\kappa n}{\delta}})$, $\Delta t = \alpha/\eta$, and $t = \Omega(\frac{\eta^2}{\epsilon\alpha\sqrt{\lambda_{\min}\|\mathbf{b}_A\|_2}})$

The high-level strategy of the proof consists of two steps. The first step is our standard conservation argument to use the ℓ_2 -norm of $\mathbf{u}(t)$ to bound the residual error at time t . Next, we show that $\mathbf{u}(t)$ will be close to \mathbf{x}^{ℓ_2} with high probability since it is doing stochastic gradient descent on f . Namely, we can infer that the $\|\mathbf{u}(t)\|_2$ is close to $\|\mathbf{x}^{\ell_2}\|_2$. Combine the two we get the convergence of the least square error $\|\mathbf{b}_A - A\mathbf{x}(t)\|_2$.

To prove the theorem, first observe that the conservation equation in (15) still holds for simple stochastic SNN. That is, we have

$$\|\mathbf{b}_A - A\mathbf{x}(t)\|_2 \leq \frac{\|\mathbf{u}(t+1)\|_2}{\sqrt{\lambda_{\min}} \cdot t \cdot \Delta t}. \quad (60)$$

Therefore, it remains to bound $\|\mathbf{u}(t+1)\|_2$. For this, we find it easier to bound $\|\mathbf{u}(t+1) - \mathbf{x}^{\ell_2}\|_2$, based on a standard approach for analyzing SGD. Note that having $\|\mathbf{u}(t+1) - \mathbf{x}^{\ell_2}\|_2 \leq \frac{\eta}{2}$ implies having $\|\mathbf{u}(t+1)\|_2 \leq \|\mathbf{u}(t+1) - \mathbf{x}^{\ell_2}\|_2 + \|\mathbf{x}^{\ell_2}\|_2 \leq \eta$. Thus, for any t , let us consider the following event:

- \mathcal{Q}_t : $\|\mathbf{u}(s) - \mathbf{x}^{\ell_2}\|_2 \leq \frac{\eta}{2}$ for every $1 \leq s \leq t$,

and our remaining task becomes to show that $\Pr[\neg\mathcal{Q}_t] \leq \delta$. As

$$\Pr[\neg\mathcal{Q}_t] \leq \sum_{s=1}^t \Pr\left[\|\mathbf{u}(s+1) - \mathbf{x}^{\ell_2}\|_2 > \frac{\eta}{2} \text{ and } \mathcal{Q}_s\right]$$

(note that $\Pr[\neg\mathcal{Q}_1] = 0$ as $\|\mathbf{u}(1) - \mathbf{x}^{\ell_2}\|_2 = \|\mathbf{x}^{\ell_2}\|_2 \leq \frac{\eta}{2}$), we then rely on the following key lemma, which we prove in Subsection 8.1.

Lemma 12. *When $\eta = \Omega(\|\mathbf{x}^{\ell_2}\|_2)$ and $\alpha = O(\frac{\eta}{\kappa\lambda_{\max}n \ln \frac{\kappa n}{\delta}})$, we have $\Pr[\|\mathbf{u}(s+1) - \mathbf{x}^{\ell_2}\|_2 > \frac{\eta}{2} \text{ and } \mathcal{Q}_s] \leq \frac{\delta}{t}$, for any $1 \leq s \leq t$.*

Combine Lemma 12 with (60) and by the choice of η and t , we have $\|\mathbf{b}_A - A\mathbf{x}(t)\|_2 \leq \epsilon \cdot \|\mathbf{b}_A\|_2$ with probability at least $1 - \delta$. This completes the proof of Theorem 4

8.1 Proof of Lemma 12

Consider any $t \leq T$. As $\mathbf{u}(t+1) = \mathbf{u}(t) - \alpha \cdot \mathbf{g}(t)$, where $\mathbf{g}(t) = A^\top A\mathbf{s}(t) - A^\top \mathbf{b} \cdot \frac{1}{\eta}$, we have

$$\|\mathbf{u}(t+1) - \mathbf{x}^{\ell_2}\|_2^2 = \|\mathbf{u}(t) - \mathbf{x}^{\ell_2}\|_2^2 - 2\alpha \langle \mathbf{g}(t), \mathbf{u}(t) - \mathbf{x}^{\ell_2} \rangle + \alpha^2 \|\mathbf{g}(t)\|_2^2.$$

Note that $\|\mathbf{g}(t)\|_2 = \|A^\top A\mathbf{s}(t) - A^\top \mathbf{b} \cdot \frac{1}{\eta}\|_2$, which is at most

$$\|A^\top A\mathbf{s}(t)\|_2 + \|A^\top \mathbf{b} \cdot \frac{1}{\eta}\|_2 \leq \lambda_{\max} \sqrt{n} + \|A^\top \mathbf{b}\|_2 \cdot \frac{1}{\eta} \leq G,$$

for $G = \sqrt{n}\lambda_{\max} + \lambda_{\max}\|\mathbf{x}^{\ell_2}\|_2 \cdot \frac{1}{\eta}$ since $\|A^\top \mathbf{b}\|_2 \leq \lambda_{\max}\|\mathbf{x}^{\ell_2}\|_2$. Moreover, $\langle \mathbf{g}(t), \mathbf{u}(t) - \mathbf{x}^{\ell_2} \rangle$ can be decomposed as

$$\langle \nabla f(\mathbf{u}(t)) \cdot \frac{1}{\eta}, \mathbf{u}(t) - \mathbf{x}^{\ell_2} \rangle - z_t, \quad \text{with } z_t = \langle \nabla f(\mathbf{u}(t)) \cdot \frac{1}{\eta} - \mathbf{g}(t), \mathbf{u}(t) - \mathbf{x}^{\ell_2} \rangle$$

such that the first term $\langle \nabla f(\mathbf{u}(t)) \cdot \frac{1}{\eta}, \mathbf{u}(t) - \mathbf{x}^{\ell_2} \rangle$ is positive due to the convexity of f as explained in the following. Since \mathbf{x}^{ℓ_2} and $\mathbf{u}(t)$ both lie in the range space of $A^\top A$, we have that

$$\begin{aligned} \langle \nabla f(\mathbf{u}(t)) \cdot \frac{1}{\eta}, \mathbf{u}(t) - \mathbf{x}^{\ell_2} \rangle &= (A^\top A\mathbf{u}(t) - A^\top \mathbf{b})^\top (\mathbf{u}(t) - \mathbf{x}^{\ell_2}) \cdot \frac{1}{\eta} \\ &= \|A\mathbf{u}(t) - \mathbf{b}_A\|_2^2 \cdot \frac{1}{\eta} \\ &= \|A(\mathbf{u}(t) - \mathbf{x}^{\ell_2})\|_2^2 \cdot \frac{1}{\eta} \\ &\geq \frac{\lambda_{\min}}{\eta} \cdot \|\mathbf{u}(t) - \mathbf{x}^{\ell_2}\|_2^2. \end{aligned}$$

Consequently, with $\gamma = 1 - \frac{2\alpha\lambda_{\min}}{\eta}$, we have

$$\|\mathbf{u}(t+1) - \mathbf{x}^{\ell_2}\|_2^2 \leq \gamma \|\mathbf{u}(t) - \mathbf{x}^{\ell_2}\|_2^2 + \alpha^2 G^2 + 2\alpha z_t,$$

and it is not hard to show by induction that

$$\begin{aligned}\|\mathbf{u}(t+1) - \mathbf{x}^{\ell_2}\|_2^2 &\leq \gamma^t \|\mathbf{u}(1) - \mathbf{x}^{\ell_2}\|_2^2 + \alpha^2 G^2 \sum_{s=0}^{t-1} \gamma^s + 2\alpha \sum_{s=0}^{t-1} \gamma^s z_{t-s} \\ &\leq \|\mathbf{x}^{\ell_2}\|_2^2 + \frac{\alpha G^2}{2\lambda_{\min}/\eta} + 2\alpha \sum_{s=0}^{t-1} \gamma^s z_{t-s}.\end{aligned}$$

As $\|\mathbf{x}^{\ell_2}\|_2^2 \leq \frac{\eta^2}{8}$ and $\frac{\alpha G^2}{2\lambda_{\min}/\eta} \leq \frac{2\alpha n \lambda_{\max}^2 + 2\alpha \lambda_{\max}^2 \|\mathbf{x}^{\ell_2}\|_2^2 \cdot \frac{1}{\eta^2}}{2\lambda_{\min}/\eta} \leq \frac{\eta^2}{8}$ for our choice of α and η , we thus have

$$\Pr \left[\|\mathbf{u}(t+1) - \mathbf{x}^{\ell_2}\|_2^2 > \frac{\eta^2}{2} \text{ and } \mathcal{Q}_t \right] \leq \Pr \left[\sum_{s=0}^{t-1} \gamma^s z_{t-s} > \frac{\eta^2}{8\alpha} \text{ and } \mathcal{Q}_t \right].$$

It remains to bound the last probability above. We would like to apply the Azuma-Hoeffding inequality for martingale difference sequence, but some care is needed.

For each $1 \leq s \leq t$, let us introduce a new random variable $\bar{\mathbf{u}}(s)$ to truncate $\mathbf{u}(s)$ when it is too large. Let $\bar{\mathbf{u}}(s)$ equals to $\mathbf{u}(s)$ if $\|\mathbf{u}(s) - \mathbf{x}^{\ell_2}\|_2 \leq \frac{\eta}{2}$ and $\mathbf{0}$ otherwise, and it gives rise to a corresponding spike vector $\bar{\mathbf{s}}(s)$, as well as the random variable \bar{z}_τ corresponding to z_τ , defined as $\langle \nabla f(\bar{\mathbf{u}}(s)) \cdot \Delta t - \nabla f(\bar{\mathbf{s}}(s)), \bar{\mathbf{u}}(s) - \mathbf{x}^*$. Then it is not hard to verify that

$$\Pr \left[\sum_{s=0}^{t-1} \gamma^s z_{t-s} > \frac{\eta^2}{8\alpha} \text{ and } \mathcal{Q}_t \right] \leq \Pr \left[\sum_{s=0}^{t-1} \gamma^s \bar{z}_{t-s} > \frac{\eta^2}{8\alpha} \right].$$

Now observe that $0, \gamma^{t-1} \bar{z}_1, \gamma^{t-2} \bar{z}_2, \dots, \bar{z}_t$ forms a martingale difference sequence with respect to $\bar{\mathbf{u}}(1), \bar{\mathbf{u}}(2), \dots, \bar{\mathbf{u}}(t)$ because for any $1 \leq s \leq t$ and $\bar{\mathbf{u}}(s)$, we always have $\|\bar{\mathbf{u}}(s)\|_2 \leq \|\bar{\mathbf{u}}(s) - \mathbf{x}^{\ell_2}\|_2 + \|\mathbf{x}^{\ell_2}\|_2 \leq \eta$ which implies that¹⁷, $\mathbb{E}[\bar{\mathbf{s}}(s) | \mathcal{F}_s] = \bar{\mathbf{u}}(s)/\eta$ and

$$\mathbb{E}[\bar{z}_s | \mathcal{F}_s] = \mathbb{E} \left[\langle \nabla f(\mathbf{u}(t)) \cdot \frac{1}{\eta} - \mathbf{g}(t), \mathbf{u}(t) - \mathbf{x}^{\ell_2} \rangle | \mathcal{F}_s \right] = 0$$

since $\Delta t = 1/\eta$. Moreover, for any $1 \leq s \leq t$,

$$\begin{aligned}|\bar{z}_s| &\leq \|\nabla f(\bar{\mathbf{u}}(s)) \cdot \frac{1}{\eta} - (A^\top A \bar{\mathbf{s}}(s) - A^\top \mathbf{b} \cdot \frac{1}{\eta})\|_2 \cdot \|\bar{\mathbf{u}}(s) - \mathbf{x}^{\ell_2}\|_2 \\ &\leq \|A^\top A(\bar{\mathbf{u}}(s) \cdot \frac{1}{\eta} - \bar{\mathbf{s}}(s))\|_2 \cdot \frac{\eta}{2} \\ &\leq \lambda_{\max} \left(\|\bar{\mathbf{u}}(s) \cdot \frac{1}{\eta}\|_2 + \|\bar{\mathbf{s}}(s)\|_2 \right) \cdot \frac{\eta}{2} \\ &\leq \lambda_{\max} \sqrt{n} \eta,\end{aligned}$$

so that we have

$$\sum_{s=0}^{t-1} (\gamma^s \bar{z}_{t-s})^2 \leq \frac{\lambda_{\max}^2 n \eta^2}{1 - \gamma} = \frac{\lambda_{\max}^2 n \eta^2}{2\alpha \lambda_{\min}/\eta}.$$

Finally, we can apply the Azuma-Hoeffding inequality and have

$$\Pr \left[\sum_{s=0}^{t-1} \gamma^s \bar{z}_{t-s} \geq \frac{\eta^2}{8\alpha} \right] \leq 2^{-\frac{\eta^4}{64\alpha^2} \cdot \frac{2\alpha \lambda_{\min}}{2\lambda_{\max}^2 n \eta^3}} \leq 2^{-\frac{\lambda_{\min} \eta}{64\alpha \lambda_{\max}^2 n}} \leq \frac{\delta}{t},$$

for our choice of α and η . This completes the proof of Lemma 12.

¹⁷ $\|\bar{\mathbf{u}}(s)\|_2 \leq \eta$ implies $|\bar{\mathbf{u}}_i(s)| \leq \eta$ for any $i \in [n]$.